

# Reassembly and co-crystallization of a family 9 processive endoglucanase from its component parts: Structural and functional significance of the intermodular linker

Svetlana Petkun, Inna Rozman Grinberg, Raphael Lamed, Sadanari Jindou, Tal Burstein, Oren Yaniv, Yuval Shoham, Linda J.W. Shimon, Edward A Bayer, Felix Frolow

Non-cellulosomal processive endoglucanase 9I (Cel9I) from *Clostridium thermocellum* is a modular protein, consisting of a family-9 glycoside hydrolase (GH9) catalytic module and two family-3 carbohydrate-binding modules (CBM3c and CBM3b), separated by linker regions. GH9 does not show cellulase activity when expressed without CBM3c and CBM3b and the presence of the CBM3c was previously shown to be essential for endoglucanase activity. Physical reassociation of independently expressed GH9 and CBM3c modules (containing linker sequences) restored 60-70% of the intact Cel9I endocellulase activity. However, the mechanism responsible for recovery of activity remained unclear. In this work we independently expressed recombinant GH9 and CBM3c with and without their interconnecting linker in *Escherichia coli*. We crystallized and determined the molecular structure of the GH9/linker-CBM3c heterodimer at a resolution of 1.68 Å to understand the functional and structural importance of the mutual spatial orientation of the modules and the role of the interconnecting linker during their re-association. Enzyme activity assays and isothermal titration calorimetry were performed to study and compare the effect of the linker on the re-association. The results indicated that reassembly of the modules could also occur without the linker, albeit with only very low recovery of endoglucanase activity. We propose that the linker regions in the GH9/CBM3c endoglucanases are important for spatial organization and fixation of the modules into functional enzymes.

1 **Reassembly and co-crystallization of a family 9 processive**  
2 **endoglucanase from its component parts:**  
3 **Structural and functional significance of the intermodular**  
4 **linker**

5  
6 Svetlana Petkun<sup>1</sup>, Inna Rozman Grinberg<sup>1</sup>, Raphael Lamed<sup>1</sup>, Sadanari Jindou<sup>2</sup>,  
7 Tal Burstein<sup>1</sup>, Oren Yaniv<sup>1</sup>, Yuval Shoham<sup>3</sup>, Linda J.W. Shimon<sup>4</sup>, Edward A.  
8 Bayer<sup>5,\*</sup>, and Felix Frolow<sup>1</sup>

9  
10 <sup>1</sup>*Department of Molecular Microbiology and Biotechnology, The Daniella Rich*  
11 *Institute for Structural Biology, Tel Aviv University, Ramat Aviv 69978 ISRAEL*

12 <sup>2</sup>*Department of Life Sciences, Meijo University, Nagoya 468-8502 JAPAN*

13 <sup>3</sup>*Department of Biotechnology and Food Engineering, Technion-Israel Institute of*  
14 *Technology, Haifa 32000 ISRAEL*

15 <sup>4</sup>*Department of Chemical Research Support and*

16 <sup>5</sup>*Department of Biological Chemistry, The Weizmann Institute of Science, Rehovot*  
17 *76100 ISRAEL*

18

19 **Corresponding author:**

Edward A. Bayer  
*Department of Biological Chemistry*  
*The Weizmann Institute of Science*  
*Rehovot 76100 ISRAEL*  
Tel: 972-8-934-2373  
Fax: 972-8-946-8256  
Email: ed.bayer@weizmann.ac.il

20

21 **Running title:** Crystal structure of reassembled Cel9I

22 **Abbreviations used:** CBM, carbohydrate-binding module; CBM3cL, family 3c CBM  
23 with linker; CBM3cNL, family 3c CBM without linker; CMC, carboxymethyl  
24 cellulose; GH9, family 9 glycoside hydrolase; ITC, isothermal titration calorimetry;  
25 PASC, phosphoric acid-swollen cellulose; SeMet, selenium-methionine labeled  
26 derivative.

27 **Abstract.**

28 Non-cellulosomal processive endoglucanase 9I (Cel9I) from *Clostridium*  
29 *thermocellum* is a modular protein, consisting of a family-9 glycoside hydrolase  
30 (GH9) catalytic module and two family-3 carbohydrate-binding modules (CBM3c and  
31 CBM3b), separated by linker regions. GH9 does not show cellulase activity when  
32 expressed without CBM3c and CBM3b and the presence of the CBM3c was  
33 previously shown to be essential for endoglucanase activity. Physical reassociation of  
34 independently expressed GH9 and CBM3c modules (containing linker sequences)  
35 restored 60-70% of the intact Cel9I endocellulase activity. However, the mechanism  
36 responsible for recovery of activity remained unclear. In this work we independently  
37 expressed recombinant GH9 and CBM3c with and without their interconnecting  
38 linker in *Escherichia coli*. We crystallized and determined the molecular structure of  
39 the GH9/linker-CBM3c heterodimer at a resolution of 1.68 Å to understand the  
40 functional and structural importance of the mutual spatial orientation of the modules  
41 and the role of the interconnecting linker during their re-association. Enzyme activity  
42 assays and isothermal titration calorimetry were performed to study and compare the  
43 effect of the linker on the re-association. The results indicated that reassembly of the  
44 modules could also occur without the linker, albeit with only very low recovery of  
45 endoglucanase activity. We propose that the linker regions in the GH9/CBM3c  
46 endoglucanases are important for spatial organization and fixation of the modules into  
47 functional enzymes.

48

49 Key words: *Clostridium thermocellum*; family-9 glycoside hydrolase; carbohydrate-  
50 binding module (CBM); X-ray structure; protein-protein interaction

51

## 52 Introduction

53 Cellulose is a major component of the plant cell wall, lending structural stability  
54 and resilience to an otherwise flaccid material. The propensity of cellulose to form  
55 ordered, tightly packed, para-crystalline fibrils hinders its enzymatic degradation.  
56 Indeed, the recalcitrant properties of cellulose are such that numerous enzymes are  
57 required to act synergistically in achieving its efficient degradation. Many types of  
58 bacteria and fungi are capable of degrading cellulose and other plant cell wall  
59 polysaccharides in an effective manner, producing a variety of various cellulases and  
60 related enzymes, either existing in the free state, or associated with a multi-enzyme  
61 complex known as the cellulosome (Bayer et al. 2004; Bayer et al. 2008; Demain et  
62 al. 2005; Doi & Kosugi 2004; Fontes & Gilbert 2010). *Clostridium thermocellum* is  
63 an anaerobic thermophilic bacterium, known for its efficient degradation of cellulose  
64 and other plant cell wall polysaccharides (Béguin et al. 1992; Freier et al. 1988;  
65 Garcia-Martinez et al. 1980; Ng et al. 1977; Wiegel et al. 1985). The cellulase system  
66 of this bacterium includes a remarkable variety of enzymes, some existing in the free  
67 state but most associated with a cellulosome (Béguin & Alzari 1998; Felix &  
68 Ljungdahl 1993; Schwarz 2001; Schwarz et al. 2004).

69 Cellulases are a class of modular enzymes with a catalytic glycoside hydrolase  
70 (GH) module that hydrolyzes the  $\beta$ -1,4-glucosidic bond of the cellulose chain  
71 (Cantarel et al. 2009; Davies & Henrissat 1995; Gilbert & Hazlewood 1993; Henrissat  
72 1991; Henrissat & Davies 1997; Wilson & Irwin 1999). The catalytic module is  
73 usually associated with various numbers of accessory modules that serve to modulate  
74 the enzyme activity, and the enzymes have been categorized into families according  
75 to the amino-acid sequence of the GH domain (Cantarel et al. 2009; Gilkes et al.  
76 1991; Henrissat & Davies 1997; Henrissat & Davies 2000; Henrissat & Romeu 1995).  
77 Cellulases have been broadly divided into two types: endoglucanases that can  
78 hydrolyze bonds internally in cellulose chain, and exoglucanases that act  
79 preferentially on chain ends, progressively cleaving off cellobiose as the main  
80 product. The distinction between endo- and exo-acting enzymes is also reflected by  
81 the architecture of the respective class of active site, whereby endoglucanases, for  
82 example, are commonly characterized by a groove or open binding cleft, into which  
83 any part of the linear cellulose chain can fit. On the other hand, the exoglucanases

84 bear tunnel-like active sites, which can only accept a substrate chain via its terminus  
85 (either the reducing or non-reducing end, depending on the enzyme), thereby cleaving  
86 cellulose in a sequential manner. The sequential hydrolysis of a cellulose chain has  
87 earned the term "processivity" (Beckham et al. 2014; Davies & Henrissat 1995;  
88 Wilson & Kostylev 2012), and processive enzymes are considered to be key  
89 components which contribute to the overall efficiency of a given cellulase system.  
90 Some endoglucanases, notably from GH family 9, have also been shown to  
91 sequentially hydrolyze cellulose chains and are thus referred to as processive  
92 endoglucanases (Gal et al. 1997; Gilad et al. 2003; Irwin et al. 1998; Jeon et al. 2012;  
93 Kuusk et al. 2015; Zverlov et al. 2003). Such enzymes appear to possess extended  
94 catalytic clefts and the observed processivity appears to require highly coordinated  
95 substrate-binding affinities from opposite sides of the cleavage site (Bu et al. 2012; Li  
96 et al. 2010; Payne et al. 2011).

97 Cellulase 9I (Cel9I), is a non-cellulosomal family 9 processive endoglucanase  
98 from *Clostridium thermocellum*, which degrades crystalline cellulose (Avicel and  
99 filter paper) as well as phosphoric acid-swollen cellulose (PASC) and carboxymethyl  
100 cellulose (CMC) (Gilad et al. 2003). This enzyme consists of a catalytic GH9 module  
101 at its N terminus, followed by two family 3 carbohydrate-binding modules (CBMs):  
102 CBM3c and CBM3b. The three modules are separated by distinctive linker sequences.  
103 Such intermodular linker segments were proposed to be important for the physical  
104 association of the modules in the space, and to promote intermodular and/or  
105 intersubunit protein–protein interactions (Bayer et al. 1998; Bayer et al. 2009; Noach  
106 et al. 2008).

107 The C-terminal CBM3b module, as a classic CBM3, is responsible for targeting  
108 the Cel9I enzyme to the planar surface of the crystalline cellulose substrate (Gilad et  
109 al. 2003; Su et al. 2012; Tormo et al. 1996). It has also been proposed to disrupt the  
110 crystalline regions of cellulose, rendering it more accessible to the GH9 catalytic  
111 module (Yi et al. 2013) and to contribute to enzyme processivity by preventing the  
112 desorption of the catalytic module from cellulose (Telke et al. 2012). The function of  
113 the CBM3c is less straightforward. Removal of CBM3c from *C. thermocellum* Cel9I  
114 and from *C. cellulolyticum* Cel9G *P. Barcinonensis* Cel9B significantly reduces the  
115 enzyme activity (Burstein et al. 2009; Chiriac et al. 2010; Gal et al. 1997). CBM3c  
116 modules have been shown to alter the normal function of the GH9 catalytic module of

117 *Thermobifida fusca* Cel9A from the standard endo-acting mode into a processive  
118 endoglucanase (Bayer et al. 1998; Irwin et al. 1998). Thus, Gilad *et al.* (Gilad et al.  
119 2003) showed in 2003 that the endoglucanase activity of Cel9I is dependent upon the  
120 presence of the CBM3c module and suggested that the fused CBM3c serves an  
121 important accessory role for the catalytic domain by altering its character to facilitate  
122 processive cleavage of recalcitrant cellulose substrates.

123 In addition to the Cel9 CBM3c, several other examples of CBMs that are  
124 considered to modulate catalytic specificity and act cooperatively with the catalytic  
125 domain have recently been discovered. These include CBM66 that directs the cognate  
126 enzyme towards highly branched glucans rather than linear fructose polymers (Cuskin  
127 et al. 2012), CBM48 that contributes to substrate binding at the active site of a glucan  
128 phosphatase (Meekins et al. 2014), family-43  $\beta$ -xylosidases where the GH43 is  
129 complemented by an additional module that confers hydrolytic activity to the mature  
130 enzyme (Moraís et al. 2012), and CBM46, that constitutes part of the catalytic cleft  
131 required for the hydrolysis of  $\beta$ -1,3-1,4-glucans (Venditto et al. 2015). The  
132 carbohydrate-binding PA14 domain is also known to affect substrate binding of the  
133 catalytic domain by contributing to the formation of its active site (Gruninger et al.  
134 2014; Zmudka et al. 2013).

135 We have previously shown that independently expressed GH9 and linker-  
136 containing CBM3c modules of Cel9I readily re-associate *in vitro* and that this  
137 physical reassociation recovers 60-70% of the intact Cel9I endoglucanase activity  
138 (Burstein et al. 2009).

139 We have examined in this work the interaction of the CBM3c with the catalytic  
140 module either with or without the intermodular linker in order to better understand the  
141 function of the CBM3c in the family-9 enzymes and the role of the linkers regions.  
142 The effect of the re-association of the CBM3c with linker (CBM3cL) and the CBM3c  
143 without linker (CBM3cNL) on the enzymatic activity of GH9 has been studied by the  
144 crystallization and structure determination of the reassembled GH9-CBM3cL  
145 complex at a resolution of 1.68 Å. The results of this study will help us to understand  
146 the contribution of ancillary modules in the action of multi-modular glycoside  
147 hydrolases.

148

## 149 **Materials and methods**

### 150 **Cloning of the GH9, CBM3cL and CBM3cNL proteins**

151 Cloning of the DNA fragments encoding the C-terminally His-tagged CBM3c with  
152 the linker and the untagged GH9 module from Cel9I of *C. thermocellum* (GenBank  
153 accession code L04735) was described earlier (Burstein et al. 2009; Gilad et al. 2003).  
154 C-terminally His-tagged CBM3c without the linker connecting it to the GH9 was  
155 amplified using the same procedure and the following primers: F' –  
156 5' CCATGGGCGAAGTTCCGGAGGATGAAATA and R' –  
157 5' CTCGAGCGGTTCCCTTCCAAATACCAG. The PCR products were purified and  
158 cleaved with restriction enzymes *NcoI* and *XhoI* and inserted into the pET-28a(+)  
159 expression vector (Novagen, Madison, WI, USA).

### 160 **Expression and purification of recombinant proteins**

161 The GH9 and CBM3c modules both with (GH9L, CBM3cL) and without (GH9NL  
162 and CBM3cNL) the linker regions were expressed independently by the identical  
163 expression procedure. *Escherichia coli* strain BL21(DE3)RIL harboring the plasmids  
164 was aerated at 310 K in 3-liters Terrific Broth supplemented with 25 mg ml<sup>-1</sup>  
165 kanamycin. After 3 h, the culture reached an A<sub>600</sub> of 0.6; 0.1 mM isopropyl-β-D-1-  
166 thiogalactopyranoside was added to induce gene expression, and cultivation was  
167 continued at 310 K for an additional 12 h. Cells were harvested by centrifugation  
168 (5,000 × g for 15 min) at 277 K and were subsequently re-suspended in 50 mM  
169 NaH<sub>2</sub>PO<sub>4</sub>, pH 8.0, containing 300 mM NaCl at a ratio of 1 g wet pellet to 4 ml buffer  
170 solution. A few micrograms of DNase powder were added prior to the sonication  
171 procedure. The suspension was kept on ice during sonication, after which it was  
172 centrifuged (20,000 × g at 277 K for 20 min), and the supernatant was collected.

173 The soluble expressed His-tagged CBM3c modules with or without the linker,  
174 according to the type of the experiment, were applied batchwise to Ni-IDA resin  
175 during 1-h incubation with gentle stirring at 4 °C. Non-specifically bound proteins  
176 were washed with a buffer containing 50 mM NaH<sub>2</sub>PO<sub>4</sub> pH 6, 300 mM NaCl, 10%  
177 glycerol and 10 mM imidazole. Crude extract supernatant fluids, containing the  
178 expressed GH9 module, were added to the CBM3c-bound Ni-IDA resin, and the  
179 mixture was incubated overnight with gentle stirring at 4 °C. The adsorbed protein

180 complexes were eluted with 300 mM imidazole and subjected to further purification  
181 by size-exclusion chromatography. Fast protein liquid chromatography (FPLC) was  
182 performed using a Superdex 75pg column and ÄKTA Prime system (GE Healthcare,  
183 Piscataway, NJ) to further purify the complex. One peak, corresponding  
184 approximately to 70 kDa, matching the predicted molecular weight of the GH9-  
185 CBM3c complex, was observed in the chromatogram. The 15 amino-acid linker  
186 sequence (about 1.5 kDa) did not significantly affect the elution volume, compared to  
187 that of the complex without the linker, presumably due to the limited resolution of the  
188 column. The relevant fractions (the purified complexed proteins) were analyzed by  
189 15% sodium dodecyl sulfate-polyacrylamide gel electrophoresis (SDS-PAGE) with  
190 Coomassie brilliant blue staining. Two clear bands, of about 52 and 19.5 kDa were  
191 observed. The rearranged modules were concentrated to 6 mg ml<sup>-1</sup> using Centriprep  
192 YM-3 centrifugal filter devices YM-3 (Amicon Bioseparation, Millipore Corporation,  
193 Bedford, USA). Protein concentration was determined by measuring UV absorbance  
194 at 280 nm.

195 The full-length Cel9I was purified by affinity chromatography on Avicel as  
196 reported earlier (Burstein et al. 2009; Gilad et al. 2003).

### 197 **Microcalorimetric analysis**

198 Isothermal titration calorimetry (ITC) experiments were carried out using a VP-  
199 ITC MicroCalorimeter (MicroCal, LLC, Northampton, MA) at 298 K. About 300 μM  
200 solution of CBM3cNL was injected into a 65 μM solution of GH9. The reaction was  
201 performed in a buffer containing 50 mM Tris-HCl, pH 7.5, 150 mM NaCl, 0.05%  
202 sodium azide. Heats of dilution of the titrants were subtracted from the titration data,  
203 and the corrected data were analyzed using the Origin ITC analysis software package  
204 supplied by MicroCal. Thermal titration data were fit to the one binding site model,  
205 and enthalpy ( $\Delta H$ ), entropy ( $\Delta S$ ), association constant ( $K_a$ ) and stoichiometry of  
206 binding ( $N$ ) were determined. In all cases, the calculated stoichiometry ( $N$ ) was lower  
207 than one, most likely due to the fact that the CBM3 proteins lost their native  
208 functionality with time. For the analysis, the CBM3 protein concentrations were  
209 corrected as to provide a stoichiometry of one. Two titrations were performed to  
210 evaluate reproducibility.

**211 Enzyme activity assay**

212 Reactions were performed at 333 K, in 50 mM citrate buffer (pH 6.0). The soluble  
213 cellulolytic substrate was carboxymethyl cellulose (CMC, Sigma Chem. Co. St.  
214 Louis, MO). The amount of reducing sugars released from the substrate was  
215 determined with the 3,5-dinitrosalicylic acid (DNS) reagent as described by Miller et  
216 al (Miller 1959). Activity was defined as the amount (micromole) of reducing sugar  
217 released after 10 min of reaction.

**218 Crystallization**

219 Initially the protein samples containing 6 mg/ml protein solution in 1.2 mM Tris-  
220 HCl pH 7.5, 1.5 mM sodium chloride, 0.025% sodium azide, were screened, using the  
221 microbatch crystallization method under 1:1 mixture of silicon and paraffin oil  
222 (Chayen et al. 1990), using 288 conditions from the Hampton Research HT screens  
223 (SaltRx, Index HT, and Crystal Screen HT; Hampton Research, Aliso Viejo, CA) and  
224 96 conditions of the Wizard Crystallization kit from Emerald BioSystems (Rigaku  
225 Reagents, Bainbridge Island, WA). The dyad of GH9 and CBM3cNL did not yield  
226 any crystals. Screening of the GH9-CBM3cL resulted in plate-like crystals that  
227 appeared after several days under several conditions, all of which contained PEG  
228 3350 and 4000. The best crystals were obtained in 30 % PEG, 0.2 M magnesium  
229 chloride, and 0.1 M HEPES, pH 7.5. Attempts to optimize this condition using  
230 microbatch, hanging-drop, and sitting drop methods were unsuccessful, as the crystals  
231 remained very thin and fragile. The superfine Eyelash (Ted Pella, Inc, Redding, CA)  
232 was used to touch these crystals and consequently to streak the sitting drops,  
233 composed of 5  $\mu$ l of the protein solution and 5  $\mu$ l of the precipitating solution (24 %  
234 PEG 3350, 0.2 M magnesium chloride, 0.1 M HEPES, pH 8.0). After one day, crystals  
235 of different morphology, with maximum size of about 0.05 mm, appeared in the drop.

**236 Data collection and crystallographic analysis**

237 The crystals of the GH9-CBM3cL complex were harvested from the crystallization  
238 drop using a nylon cryo-loop (Hampton Research, Aliso Viejo, CA). For data  
239 collection, crystals were mounted on the MiTeGen stiff micro-mount (MiTeGen,  
240 Ithaca, NY) made of polyimide and flash-cooled in a nitrogen stream produced by  
241 Oxford Cryostream low temperature generator (Cosier & Glazer 1986) at a

242 temperature of 100 K. Mother-liquor of the crystals served for cryo-protection during  
243 the cooling in liquid nitrogen.

244 Diffraction data from the GH9-CBM3cL crystals were measured using the ID23-2  
245 beam line at ESRF, Grenoble, France. A MAR CCD 225 area detector and X-ray  
246 radiation of 0.873 Å wavelength were used. Diffraction data of 480 images with 0.5°  
247 oscillation per image were collected. Data were processed with *DENZO* and scaled  
248 with *SCALEPACK* as implemented in *HKL2000* (Otwinowski & Minor 1997). The  
249 crystals diffracted to 1.68 Å resolution and belong to the orthorhombic space group  
250  $P2_12_12_1$ , with unit cell parameters  $a=70.4$ ,  $b=88.5$ ,  $c=106.5$  Å. There is one GH9-  
251 CBM3cL complex per asymmetric unit with a Matthews density  $V_M$  of  $2.37 \text{ \AA}^3 \text{ Da}^{-1}$ ,  
252 corresponding to a solvent content of 48.15% (Matthews 1968). The X-ray data  
253 analysis statistics are presented in Table 1 (Stout & Jensen 1968).

254 Molecular replacement was carried out with *MOLREP* (Vagin & Teplyakov 1997),  
255 using the coordinates of the GH9 and CBM3c modules of endoglucanase 9G from  
256 *Clostridium cellulolyticum* (PDB code 1G87, 66 and 51% sequence identity,  
257 respectively), as a search model. The *MOLREP* calculations with the GH9 domain  
258 converged into a clear solution with 1 molecule in the asymmetric unit with an R-  
259 factor of 0.533 and correlation coefficient of 0.567. This solution was inserted into  
260 *MOLREP* calculations as a fixed molecule and the coordinates of CBM3c module  
261 were used for the search producing a solution with an  $R_{\text{cryst}}$  of 0.505, and correlation  
262 coefficient of 0.582. The resulting model with 5% of reflections forming test set  
263 (Brünger 1992) was subjected to 10 cycles of restrained refinement using anisotropic  
264 B-factors, yielding the  $R_{\text{cryst}}$  and  $R_{\text{free}}$  0.329 and 0.359, respectively (*REFMAC5*)  
265 (Murshudov et al. 1997). Automated model building by *ARP/wARP* (Perrakis et al.  
266 1999) produced a complete structure with  $R_{\text{cryst}}$  and  $R_{\text{free}}$  of 0.218 and 0.243  
267 respectively. The model was manually corrected using *COOT* (Emsley & Cowtan  
268 2004) and refined using *REFMAC5* (Murshudov et al. 1997). The  $R_{\text{cryst}}$  and  $R_{\text{free}}$   
269 improved to 0.184 and 0.228, respectively. Solvent atoms were built using *ARP/warp*  
270 (Perrakis et al. 1999). Refinement of TLS (rigid body translation/libration/screw  
271 motions) parameters was performed (Winn et al. 2001; Winn et al. 2003). The model  
272 was subjected to several additional cycles of manual rebuilding and refinement. The  
273 model converged to final  $R_{\text{cryst}}$  and  $R_{\text{free}}$  factors of 0.144 and 0.176, respectively.

274 The refinement statistics of the structure are summarized in Table 2. The structure  
275 was validated using *MolProbity* (Davis et al. 2007).

## 276 Protein sequence analysis

277 Sequence alignments were performed using *CLUSTALW* (Larkin et al. 2007) and  
278 the coloring of residues (representing degree of conservation) using ProtSkin (Deprez  
279 et al. 2005). Sources of the sequences used in this work are as follows: *Clostridium*  
280 *thermocellum* Cel9I GH9 module, CBM3c and CBM3b (AAA20892.1); *Clostridium*  
281 *cellulolyticum* Cel9G GH9 module, CBM3c (AAA73868.1); *Thermobifida fusca*  
282 Cel9A GH9 module and CBM3c (AAB42155.1); *Cellulomonas fimi* Ce9A CBM3c  
283 (AAA23086.1); *Clostridium cellulovorans* EngH CBM3c (AAC38572.2) and CbpA  
284 CBM3a (AAA23218.1); *Clostridium stercorarium* CelZ CBM3c and CBM3b  
285 (CAA39010.1) and CelY CBM3b (CAA93280.1); *Clostridium thermocellum* CipA  
286 CBM3a (CAA48312.1), CelQ CBM3c (BAB33148.1), Cel9V CBM3c' and CBM3b'  
287 (CAK22315.1), Cel9U CBM3c' and CBM3b' (CAK22317.1) and Cbh9A CBM3b  
288 (CAA56918.1); *Clostridium cellulolyticum* CipC CBM3a (AAC28899.2) and CelJ  
289 CBM3c (AAG45158.1); *Acetivibrio cellulolyticus* Cel9B CBM3c' and CBM3b'  
290 (CAI94607.1) and CipV (ScaA) CBM3b (AAF06064.1); *Clostridium josui* CipA  
291 (CipJ) CBM3a (BAA32429.1); *Bacteroides cellulosolvans* ScaA CBM3b  
292 (AAG01230.2); *Bacillus subtilis* CelA CBM3b (AAA22307.1); *Pectobacterium*  
293 *atrosepticum* CelVI CBM3b (X79241.2); *Bacillus licheniformis* CelA CBM3b  
294 (CAJ70714.1).

295

296

## 297 Results

### 298 Cloning, expression and purification of Cel9I and its modular 299 components

300 The full-length *C. thermocellum* Cel9I enzyme and its individual component parts  
301 were over-expressed in *Escherichia coli*, according to Burstein et al (2009), in order  
302 to investigate the contribution of the ancillary modules and their linkers to the  
303 catalytic activity of the enzyme. These include the isolated GH9 module with and  
304 without a His tag, the His-tagged CBM3c module together with its adjacent N-

305 terminal linker that connects it to the GH9 module (CBM3cL) and His-tagged CBM3c  
306 module without the N-terminal linker (CBM3cNL). For details, see Figure 1.  
307 Following purification procedures, all recombinant proteins showed a single band in  
308 SDS-PAGE of the anticipated molecular masses.

### 309 **Recovery of endoglucanase activity upon association of CBM3cNL and** 310 **GH9 compared to CBM3cL and GH9**

311 Previous works (Burstein et al. 2009; Gilad et al. 2003) demonstrated that the  
312 Cel9I catalytic module alone has no detectable activity on CMC (carboxymethyl  
313 cellulose) and that adding the CBM3cL to form the Cel9I-CBM3cL-CBM3b triad  
314 serves to recover up to 70% of the lost activity. To further examine the importance of  
315 the linker connecting the GH9 and the CBM3c modules, we tested the ability of  
316 CBM3cNL to recover the CMCase activity of GH9. A fixed amount of the catalytic  
317 module (70 pmol in 400  $\mu$ l) was mixed with increasing amounts of CBM3cL or  
318 CBM3cNL. The activity of the intact Cel9I enzyme was defined as 100%, and the  
319 activity of the reconstituted complexes was measured relative to that of Cel9I. The  
320 results indicated that GH9-CBM3cNL exhibit only about 10% of the intact Cel9I  
321 activity towards CMC, whereas the reassembled GH9-CBM3cL provided up to 50%  
322 of the activity (Figure 2). The fact that a higher than one molar ratio was required to  
323 obtain maximum activity can be explained by the fact that the CBM protein was only  
324 partly functional as was also observed in the ITC experiments described below.  
325 Overall the results suggest that the linker is required for better fitting of the  
326 reconstituted CBM3c which results in better recovered activity.

### 327 **Overall structure of the reassembled GH9-CBM3c**

328 The crystal structure of the reassembled *C. thermocellum* Cel9I GH9-CBM3cL  
329 dyad was determined by molecular replacement and the coordinates are deposited in  
330 Protein Data Bank with code 2XFG. Data collection and refinement statistics are  
331 given in Tables 1 and 2. The catalytic GH9 and the ancillary CBM3c modules  
332 reassembled in vitro to form a dyad (Figure 3a) similar in structure to the intact  
333 tandem GH9-CBM3c modules of the orthologous endoglucanases: Cel9G from *C.*  
334 *cellulolyticum* (1G87) and Cel9A (previously termed cellulase E4) from *Thermobifida*  
335 *fusca* (1TF4), with an RMS deviation of 0.783 Å over 468 C $\alpha$  atoms with Cel9G and  
336 0.757 Å with Cel9A (Figure 3b).

337 **Structure of the GH9 module**

338 The catalytic module of the Cel9I enzyme consists of residues 1-446, comprising  
339 15  $\alpha$ -helices, whereby the twelve longest ones form the  $(\alpha/\alpha)_6$ -barrel (Figure 4A).  
340 The hydrophobic core of the GH9 module is formed by 118 hydrophobic and  
341 aromatic amino acids, the vast majority of which are also conserved in the GH9  
342 modules from *C. cellulolyticum* Cel9G and *T. fusca* Cel9A. Hydrophobic and  
343 aromatic cores have been proposed to play an important role in the formation of  
344  $(\alpha/\alpha)_6$ -barrels (Mandelman et al. 2003). The GH9 module of Cel9I thus shows high  
345 structural similarity with the two latter GH9 structures: *C. cellulolyticum* Cel9G  
346 (0.367 Å RMS deviation over 349 C-alpha atoms) and *T. fusca* Cel9A (0.532 Å RMS  
347 deviation over 359 C-alpha atoms).

348 The catalytic site of the GH9 module is located at the depression in the flat surface,  
349 formed by the loops connecting the N termini of the barrel helices (Figure 4B). The  
350 flat face is rich in charged and polar residues (Figure 4B), highly conserved also in  
351 Cel9G (1G87) and Cel9A (1TF4). The GH9 modules of these cellulases (Mandelman  
352 et al. 2003; Sakon et al. 1997; Zhou et al. 2004) exhibit similar flat faces and clefts,  
353 and these conserved residues (His 126, Trp 129, Phe 205, Tyr 206, Trp 209, Trp 256,  
354 Asp 261, Asp 262, Trp 314, Arg 318, His 376, Arg 378, and Tyr 419) have been  
355 shown to bind natural and synthetic oligosaccharides (Figure 4C). In the present  
356 structure, as in the other known GH9-CBM3c bimodular structures, one end of this  
357 cleft is blocked by a loop formed by residues 243-254 and the other end is fused with  
358 the flat surface of the CBM3c module (Figure 4B). Details of the catalytic cleft are  
359 presented in Figure 4C.

360 One calcium ion is found near the catalytic cleft of the GH9 module of Cel9I and is  
361 coordinated by a Ser 210 (OG) 2.6 Å, Gly 211 (O) 2.4 Å, Asp 261 (O) 2.4 Å, Asp 214  
362 bifurcated (OD1, OD2) 2.5 Å, and Glu 215 bifurcated (OD1, OD2) 2.5 Å (Figure  
363 4D). Despite some minor changes in the residues of coordination this ion seems to be  
364 structurally equivalent to those of *T. fusca* Cel9A (RMS deviation 0.160 Å over 5 C $\alpha$   
365 atoms of the coordinating residues), and *C. cellulolyticum* Cel9G (RMS deviation  
366 0.503 Å over 4 C $\alpha$  atoms). In all three cases the calcium ion draws together the N-  
367 terminal ends of  $\alpha$ -helices 8 and 10.

368 **Structure of the CBM3c module**

369 The CBM3c module consists of 150 amino acids arranged in an eight  $\beta$ -stranded  
370 sandwich motif homologous to other known family 3 CBM structures (Gilbert et al.  
371 2013; Mandelman et al. 2003; Petkun et al. 2010b; Sakon et al. 1997; Shimon et al.  
372 2000b; Tormo et al. 1996; Yaniv et al. 2014; Yaniv et al. 2012b; Yaniv et al. 2011).  
373 The “lower” face of the sandwich is formed by  $\beta$ -strands 1, 2, and 7; the “upper” face  
374 is formed by  $\beta$ -strands 3, 3', 6, 8, and 9 (Figure 5A). The structure of Cel9I CBM3c is  
375 particularly similar to the structures of the other two previously described CBM3c  
376 structures (RMS deviation 0.734 Å over 116 C-alpha atoms with CBM3c from *C.*  
377 *cellulolyticum* Cel9G; RMS deviation 0.829 Å over 113 atoms with CBM3c from *T.*  
378 *fusca* Cel9A). Only 31% of amino acids are located in  $\beta$ -strands of the CBM3c  
379 module from Cel9I; others are found in the loop regions.

380 One calcium ion was found in the upper  $\beta$ -sheet of the CBM3c molecule (Figure  
381 5B) and is coordinated by a water molecule and five residues from the upper  $\beta$ -sheet:  
382 Asn 500 (O), Glu 503 bifurcated (OE1, OE2), Asn 573 (O), Asn 576 (OD1), Asp 577  
383 (OD1). This calcium atom is in a similar location as in Cel9A and Cel9G, and  
384 probably plays a structural role for most CBM3 modules, as was suggested previously  
385 (Tormo et al. 1996).

386 The lower sheet forms a flat platform conserved between the CBM3c modules and  
387 the other two molecular structures. This flat surface is rich in charged and polar  
388 conserved surface residues: Asn 466, Glu 474, Lys 476, Ser 518, Tyr 520, Glu 559,  
389 Gln 561, and Arg 563 (Figure 5C). The planar region of the CBM3c modules in all  
390 three enzymes is particularly aligned in continuation of the catalytic cleft of the  
391 catalytic modules, and has been proposed to bind single chains of cellulose and guide  
392 them to the cleft (Mandelman et al. 2003; Sakon et al. 1997).

393 The CBM3c possesses a very interesting surface structure, formed by the  $\beta$ -strands  
394 on the opposite side of the flat surface, called the “shallow groove” (Shimon et al.  
395 2000b; Tormo et al. 1996). The “shallow groove” is lined by four aromatic rings (Phe  
396 498, Tyr 538, Tyr 578 and Tyr 597), two charged or polar residues (Arg 496, and Glu  
397 540), Leu 602, Pro 595 and Pro 608. These residues are also conserved in other  
398 CBM3 modules regardless of their subgroup relation (a, b, or c), their cellulose-  
399 binding ability and their effect on the activity of the catalytic module. Figure 5D  
400 shows the shallow groove of the CBM3c module from the Cel9I enzyme colored

401 according to the extent of the conservation of the residues in other CBM3a, b and c  
402 modules (darker blue represents more conservation). The alignment was performed  
403 over 25 CBM3 sequences (11 CBM3c, 12 CBM3b and CBM3b', and 4 CBM3a).  
404 Conservation of this surface structure, regardless of the particular known function of  
405 the CBMs, implies that this site has some kind of "generic" function. This shallow  
406 groove may serve to bind to single oligosaccharide chains or to peptide chains, such  
407 as the intermodular linkers common to cellulases or cellulosomal scaffoldin subunits.  
408 There is evidence that the shallow groove interacts with a linker region (Petkun et al.  
409 2010a; Shimon et al. 2000a; Yaniv et al. 2012a).

#### 410 **Contact residues between the GH9, linker and CBM3c**

411 The *in vitro* reassembled GH9-CBM3cL complex has a large intermodular  
412 interface, the contact area of which is 1108.3 Å<sup>2</sup>, corresponding to 12.3% of the total  
413 surface-exposed area of the CBM3c module and 6.2% of the exposed GH9 module  
414 (Krissinel & Henrick 2007). The GH9 and the CBM3cL modules of Cel9I are  
415 assembled into the reconstituted GH9-CBM3c complex by 31 hydrogen bonds (4  
416 main chain-main chain, 19 main chain-side chain, and 8 side chain-side chain), 14  
417 hydrophobic, 3 aromatic interactions, and 3 ionic bonds  
418 (<http://pic.mbu.iisc.ernet.in/index.html>) (Tina et al. 2007). Sixteen residues from the  
419 GH9 module and seventeen residues from the CBM3c participate in these interactions  
420 (contact residues are shown in Figure 6A). The vast majority of the contact residues  
421 and contacts are similar to those of *C. cellulolyticum* Cel9G and of *T. fusca* Cel9A  
422 (Figure 6B). Conserved residues of the linker make contacts with conserved residues  
423 of the GH9 module, emphasizing the importance of the linker in this interaction.

424 As mentioned above, the mutual spatial orientation of the GH9 and CBM3c  
425 modules is very similar to that in the native, intact bimodular pairs from Cel9G and  
426 Cel9A leading to the overall similarity in structures. The remarkable conservation of  
427 the overall architecture in the reassembled *in vitro* complex together with the striking  
428 conservation of the contact residues implies its high functional importance. In all of  
429 these structures (Cel9G, Cel9A, and the reassembled GH9-CBM3cL from Cel9I), the  
430 flat surface of the CBM3c module is aligned in continuation with the catalytic cleft of  
431 the GH9 module, making an extended platform (Figure 4B). This platform is rich in  
432 charged and polar surface residues that are highly conserved throughout the family 3  
433 CBMc's.

434 **Microcalorimetric analysis of the GH9-CBM3c complex formation**

435 The binding constants of GH9 and the CBM3c were obtained by performing  
436 isothermal titration calorimetry (ITC) experiments in which a solution of GH9 was  
437 titrated with a solution of CBM3c with or without the linker (Figure 7). Control  
438 experiments for each of the components alone were conducted and subtracted from  
439 the titration data. In both cases the titration curve could be fitted to a one-site  
440 binding model although the calculated stoichiometry was less than one. The low  
441 stoichiometry is probably a result of the fact that the soluble CBM module lost its  
442 functionality with time and its true active concentration was less than the measured  
443 protein concentration. To estimate the binding constants for the two CBM3c forms  
444 the CBM3c concentrations were corrected to provide a stoichiometry of one. In all  
445 cases the binding reactions were enthalpy driven with a negative entropy contribution.  
446 CBM3cL provided binding constants ( $K_d$ ) between  $1.3\text{-}2.0 \times 10^{-6}$  M, whereas  
447 CBM3cNL exhibited stronger binding constants,  $K_d$  between  $2.9\text{-}4.3 \times 10^{-7}$  M. Thus,  
448 the linker may serve as a mitigating factor for the binding process, ensuring specific  
449 binding orientation. This is consistent with the structural data and the activity assays,  
450 which emphasizes the important role of the linker in enzyme functioning. In the case  
451 of CBM3cNL, the binding process may occur faster in the absence of linker, but may  
452 also lead to unspecific binding and aggregation of the modules.

453

454

455 **Discussion**

456 A striking feature of the family 9 glycoside hydrolases is their subdivision into  
457 architectural themes, which are defined by their conserved modular composition  
458 (Bayer et al. 2006). In this context, the Theme B1 endoglucanases contain a GH9  
459 catalytic module followed by a purportedly fused family 3c CBM. Biochemical  
460 studies of some of the members of this group (Arai et al. 2001; Chiriac et al. 2010;  
461 Gal et al. 1997; Irwin et al. 1998; Li et al. 2007) have shown that the CBM3c acts as a  
462 modulator of the function of the catalytic module. However, the exact manner in  
463 which the CBM3c functions is still unclear. It has been shown (Gal et al. 1997; Gilad  
464 et al. 2003; Irwin et al. 1998) that family 3c CBMs (including the CBM3c from *C.*  
465 *thermocellum* Cel9I) fail to bind insoluble cellulosic substrates, implying that they do

466 not act as targeting agents for such substrates. The targeting of the enzyme to  
467 crystalline cellulose is achieved either through an additional CBM (Kostylev et al.  
468 2012) or by attachment of the enzyme to a CBM-containing scaffoldin via a cohesin-  
469 dockerin interaction (Mingardon et al. 2011).

470

471 The CBM3c module of Cel9A from the *T. fusca* has been proposed to loosely  
472 anchor the enzyme to cellulose, to disrupt the hydrogen bonds in crystalline cellulose  
473 and to guide a single cellulose strand towards the active site of the GH9 catalytic  
474 module (Bayer et al. 2006; Li et al. 2007). This hypothesis has been supported by  
475 molecular docking and molecular dynamics simulation studies (Oliveira et al. 2009).  
476 Moreover, double point mutations indicated that high coordination between the  
477 substrate affinities of the catalytic module and CBM needs to be precisely controlled  
478 (Li et al. 2010). Enzyme thermostability was reported to be affected by the presence  
479 of the CBM3c probably due to the formation of a compact structure (Chiriac et al.  
480 2010; Su et al. 2012; Yi et al. 2013).

481

482 The previously reported structures of Cel9A from *T. fusca* (Sakon et al. 1997)  
483 and Cel9G from *C. cellulolyticum* (Mandelman et al. 2003) revealed that the catalytic  
484 module and the CBM3c are separated by a ~20-residue linker that forms multiple  
485 polar and hydrophobic interactions mainly with the GH9 module. In an earlier report,  
486 we demonstrated that separately expressed GH9 and CBM3cL from Cel9I of *C.*  
487 *thermocellum* interact with one another to form an enzymatically active complex  
488 (Burstein et al. 2009). In the current article, we showed further that the GH9 and  
489 CBM3c can also be reassembled without the linker, albeit at the expense of catalytic  
490 activity, thus emphasizing the importance of the linker in positioning correctly the  
491 CBM relative to the GH9 catalytic module.

492

493 There is evidence that linkers in multi-modular proteins may serve  
494 communication roles between the modules via allosteric mechanisms and variation in  
495 their sequences affect enzyme activity (Ma et al. 2011). Linker length and rigidity was  
496 shown to play a critical role in the cooperative action of the catalytic module of a  
497 cellulase and a CBM (Ting et al. 2009). Computational studies of *T. fusca* Cel9A  
498 suggested that thermal contributions to enzyme plasticity and molecular motion at

499 high temperatures may play a role in enhancing CBM and catalytic domain synergy,  
500 and the linker may have an important role in this process (Batista et al. 2011). The  
501 length of the linkers may also play an important role in protein function and  
502 adaptation to the environment (Sonan et al. 2007). Studies in cellulolytic fungi  
503 revealed that linkers undergo modifications such as glycosylation and have also been  
504 shown to directly bind to the cellulose substrate (Beckham et al. 2012; Payne et al.  
505 2013; Sammond et al. 2012; Srisodsuk et al. 1993). Point mutations in different  
506 fungal GH-CBM linkers have also been shown to significantly affect the activity of  
507 the enzymes and their stability (Couturier et al. 2013; Lu et al. 2014).

508

509         The characteristics of the reassembled linker-containing complex are  
510 corroborated by the X-ray crystallographic data. Indeed, it is quite surprising that the  
511 two separately expressed entities recombined in such a way that the complex could in  
512 fact be crystallized. Moreover, the resultant structure was remarkably similar to the  
513 known structures of the intact bimodular GH9-CBM3c pairs from *C. cellulolyticum*  
514 Cel9G and *T. fusca* Cel9A. Accordingly, the vast majority of the contact residues are  
515 similar among the three structures. Conserved residues of the linker make contacts  
516 with conserved residues of the GH9 module, highlighting the importance of the linker  
517 in this interaction. The similarity of the reassembled and native intact structures is  
518 particularly intriguing, as it suggests that folding of the modular structures and  
519 emplacement of the linker during biosynthesis and intermodular recognition during  
520 complex formation are governed by the same interactions, which may have distinct  
521 functional consequences. In contrast to the GH9-CBM3c<sub>L</sub>, the re-associated GH9-  
522 CBM3c<sub>NL</sub> complex never crystallized, suggesting that the reassembly of the two  
523 modules in the absence of linker was somewhat heterogeneous in character.

524

525         Single proteins commonly fold into defined structures, wherein their N- and C-  
526 terminal ends are in relatively close proximity to one another. If we view the  
527 structures of the Theme B1 enzymes, it is evident that their individual modules, the  
528 GH9 catalytic module and the CBM3c, are consistent with this rule. The positions of  
529 the N- and C-termini of the Theme B1 catalytic module are similar to those of the  
530 other GH9 thematic members, including those of Theme A, which lack additional  
531 modules. Likewise, the N- and C-termini of CBM3c are essentially the same as all

532 other members of the family 3 CBMs, regardless of their source (i.e., parent cellulase,  
533 scaffoldin, etc). The evolutionary significance of this observation is that, originally,  
534 the functional relationship between the two modules was likely a more conventional  
535 one, whereby an ancestral CBM3 played a standard targeting role to deliver the GH9  
536 catalytic module to its substrate. During the course of evolution, this relationship  
537 changed, and the precise positioning and fusion of a mutated CBM3 with a GH9  
538 catalytic module served to modulate the activity characteristics of the latter. For this  
539 purpose, the flat surface of the CBM3c is aligned with the flat surface of the catalytic  
540 module, and the appropriate residues that interact with the single cellulose chain are  
541 thus aligned with the active site of the GH9 module. As a consequence, the two  
542 closely juxtaposed modules can be considered as a single functional entity. The  
543 functional positioning and fusion of the two modules, however, are at odds with the  
544 inherent locations of the termini of the two modules, such that the C-terminus of the  
545 catalytic module is very distant from the N-terminus of the CBM3c. Consequently,  
546 nature has provided a very distinctive type of conserved linker, which both connects  
547 the two modules and helps secure their required orientation for processive  
548 endoglucanase activity.

549

## 550 **Conclusions**

551 Cellulase 9I (Cel9I), a non-cellulosomal family 9 processive endoglucanase from  
552 *Clostridium thermocellum*, which degrades crystalline cellulose phosphoric acid-  
553 swollen cellulose (PASC) and carboxymethyl cellulose (CMC), consists of a catalytic  
554 GH9 module followed by two family 3 carbohydrate-binding modules (CBMs):  
555 CBM3c and CBM3b, separated by linker regions. C-terminal CBM3b module, as a  
556 classic CBM3, is responsible for targeting the Cel9I enzyme to the planar surface of  
557 the crystalline cellulose. The CBM3c is crucial for the GH9 enzymatic activity. In this  
558 work we investigated the interaction of separately expressed catalytic module and  
559 CBM3c either with or without the intermodular linker in order to better understand  
560 the function of the CBM3c in the family-9 enzymes and the role of the linkers  
561 regions.  
562 GH9 catalytic module and CBM3c were able to interact and reassemble both with and  
563 without the linker; however the linker was essential for the endoglucanase catalytic  
564 activity. Surprisingly, we were able to crystallize these two separately expressed

565 entities, meaning that their reassembly was very ordered and structurally  
566 homogeneous. The molecular structure of the GH9 and CBM3c with the linker region  
567 showed that they form a complex similar in structure to the intact tandem GH9-  
568 CBM3c modules of the orthologous endoglucanases Cel9G from *C. cellulolyticum*  
569 and Cel9A from *Thermobifida fusca*. The flat, conserved surface of the CBM3c  
570 module is aligned in continuation with the catalytic cleft of the GH9 module,  
571 presumably forming one functional entity, which binds to the planar surface of the  
572 cellulose. Conserved residues of the linker make contacts with conserved residues of  
573 the GH9 module, highlighting the importance of the linker in this interaction. Overall  
574 our results demonstrate that the linker regions in the GH9/CBM3c endoglucanases are  
575 necessary to achieve the right spatial organization of the modules and for the fixation  
576 of the modules into functional enzymes.

577

## 578 **Acknowledgements**

579 This article is dedicated to the memory of Professor Felix Frolow, who passed away  
580 on 29 August 2014. We thankfully acknowledge the ESRF for synchrotron beam time  
581 and staff scientists of the ID-29 beam line for their assistance.

582

583 **References**

- 584 Arai T, Ohara H, Karita S, Kimura T, Sakka K, and Ohmiya K. 2001. Sequence of  
585 celQ and properties of celQ, a component of the *Clostridium thermocellum*  
586 cellulosome. *Appl Microbiol Biotechnol* 57:660-666.
- 587 Batista PR, de Souza Costa MG, Pascutti PG, Bisch PM, and de Souza W. 2011. High  
588 temperatures enhance cooperative motions between CBM and catalytic  
589 domains of a thermostable cellulase: mechanism insights from essential  
590 dynamics. *Physical Chemistry Chemical Physics* 13:13709-13720.
- 591 Bayer EA, Belaich J-P, Shoham Y, and Lamed R. 2004. The cellulosomes: Multi-  
592 enzyme machines for degradation of plant cell wall polysaccharides. *Annu Rev*  
593 *Microbiol* 58:521-554.
- 594 Bayer EA, Lamed R, White BA, and Flint HJ. 2008. From cellulosomes to  
595 cellulosomes. *Chem Rec* 8:364-377.
- 596 Bayer EA, Morag E, Lamed R, Yaron S, and Shoham Y. 1998. Cellulosome structure:  
597 four-pronged attack using biochemistry, molecular biology, crystallography  
598 and bioinformatics. In: Claeysens M, Nerinckx W, and Piens K, eds.  
599 *Carbohydrases from Trichoderma reesei and other microorganisms*. London:  
600 The Royal Society of Chemistry, 39-65.
- 601 Bayer EA, Shoham Y, and Lamed R. 2006. Cellulose-decomposing prokaryotes and  
602 their enzyme systems. In: Dworkin M, Falkow S, Rosenberg E, Schleifer K-H,  
603 and Stackebrandt E, eds. *The Prokaryotes, Third Edition*. New York:  
604 Springer-Verlag, 578-617.
- 605 Bayer EA, Smith SP, Noach I, Alber O, Adams JJ, Lamed R, Shimon LJW, and  
606 Frolow F. 2009. Can we crystallize a cellulosome? In: Sakka K, Karita S,  
607 Kimura T, Sakka M, Matsui H, Miyake H, and Tanaka A, eds. *Biotechnology*  
608 *of lignocellulose degradation and biomass utilization*: Ito Print Publishing  
609 Division, 183-205.
- 610 Beckham GT, Dai Z, Matthews JF, Momany M, Payne CM, Adney WS, Baker SE,  
611 and Himmel ME. 2012. Harnessing glycosylation to improve cellulase  
612 activity. *Curr Opin Biotechnol* 23:338-345.
- 613 Beckham GT, Stahlberg J, Knott BC, Himmel ME, Crowley MF, Sandgren M, Sorlie  
614 M, and Payne CM. 2014. Towards a molecular-level theory of carbohydrate  
615 processivity in glycoside hydrolases. *Curr Opin Biotechnol* 27:96-106.
- 616 Béguin P, and Alzari PM. 1998. The cellulosome of *Clostridium thermocellum*.  
617 *Biochem Soc Trans* 26:178-185.
- 618 Béguin P, Millet J, and Aubert J-P. 1992. Cellulose degradation by *Clostridium*  
619 *thermocellum*: From manure to molecular biology. *FEMS Microbiol Lett*  
620 100:523-528.
- 621 Brünger TA. 1992. Free R value: a novel statistical quantity for assessing the  
622 accuracy of crystal structures. *Nature* 355:472-475.
- 623 Bu L, Nimlos MR, Shirts MR, Stahlberg J, Himmel ME, Crowley MF, and Beckham  
624 GT. 2012. Product binding varies dramatically between processive and  
625 nonprocessive cellulase enzymes. *J Biol Chem* 287:24807-24813.
- 626 Burstein T, Shulman M, Jindou S, Petkun S, Frolow F, Shoham Y, Bayer EA, and  
627 Lamed R. 2009. Physical association of the catalytic and helper modules of a  
628 processive family-9 glycoside hydrolase is essential for activity. *FEBS Lett*  
629 583:879-884.

- 630 Cantarel BL, Coutinho PM, Rancurel C, Bernard T, Lombard V, and Henrissat B.  
631 2009. The Carbohydrate-Active Enzymes database (CAZy): an expert  
632 resource for glycomics. *Nucl Acids Res* 37:D233-238.
- 633 Chayen NE, Shaw Stewart PD, Maeder DL, and Blow DM. 1990. An automated  
634 system for micro-batch protein crystallization and screening. *J Appl*  
635 *Crystallogr* 23:297-302.
- 636 Chiriac AI, Cadena EM, Vidal T, Torres AL, Diaz P, and Pastor FI. 2010.  
637 Engineering a family 9 processive endoglucanase from *Paenibacillus*  
638 *barcinonensis* displaying a novel architecture. *Applied microbiology and*  
639 *biotechnology* 86:1125-1134.
- 640 Cosier J, and Glazer AM. 1986. A nitrogen-gas-stream cryostat for general X-ray-  
641 diffraction studies. *J Appl Crystallogr* 19:105-107.
- 642 Couturier M, Feliu J, Bozonnet S, Roussel A, and Berrin JG. 2013. Molecular  
643 engineering of fungal GH5 and GH26 beta-(1,4)-mannanases toward  
644 improvement of enzyme activity. *PLoS one* 8:e79800.
- 645 Cuskin F, Flint JE, Gloster TM, Morland C, Basle A, Henrissat B, Coutinho PM,  
646 Strazzulli A, Solovyova AS, Davies GJ, and Gilbert HJ. 2012. How nature can  
647 exploit nonspecific catalytic and carbohydrate binding modules to create  
648 enzymatic specificity. *Proceedings of the National Academy of Sciences of the*  
649 *United States of America* 109:20889-20894.
- 650 Davies G, and Henrissat B. 1995. Structures and mechanisms of glycosyl hydrolases.  
651 *Structure* 3:853-859.
- 652 Davis IW, Leaver-Fay A, Chen VB, Block JN, Kapral GJ, Wang X, Murray LW,  
653 Arendall WB, 3rd, Snoeyink J, Richardson JS, and Richardson DC. 2007.  
654 MolProbity: all-atom contacts and structure validation for proteins and nucleic  
655 acids *Nucl Acids Res* 35(Web Server issue):W375-383.
- 656 Demain AL, Newcomb M, and Wu JH. 2005. Cellulase, clostridia, and ethanol.  
657 *Microbiol Mol Biol Rev* 69:124-154.
- 658 Deprez C, Llobes R, Gavioli M, Marion D, Guerlesquin F, and Blanchard L. 2005.  
659 Solution structure of the *E. coli* TolA C-terminal domain reveals  
660 conformational changes upon binding to the phage g3p N-terminal domain *J*  
661 *Mol Biol* 346:1047-1057.
- 662 Doi RH, and Kosugi A. 2004. Cellulosomes: plant-cell-wall-degrading enzyme  
663 complexes. *Nat Rev Microbiol* 2:541-551.
- 664 Emsley P, and Cowtan K. 2004. Coot: model-building tools for molecular graphics.  
665 *Acta Crystallographica Section D-Biological Crystallography* 60:2126-2132.
- 666 Felix CR, and Ljungdahl LG. 1993. The cellulosome - the exocellular organelle of  
667 *Clostridium*. *Annu Rev Microbiol* 47:791-819.
- 668 Fontes CM, and Gilbert HJ. 2010. Cellulosomes: Highly efficient nanomachines  
669 designed to deconstruct plant cell wall complex carbohydrates. *Annu Rev*  
670 *Biochem* 79:655-681.
- 671 Freier D, Mothershed CP, and Wiegel J. 1988. Characterization of *Clostridium*  
672 *thermocellum* JW20. *Appl Environ Microbiol* 54:204-211.
- 673 Gal L, Gaudin C, Belaich A, Pagès S, Tardif C, and Belaich J-P. 1997. CelG from  
674 *Clostridium cellulolyticum*: a multidomain endoglucanase acting efficiently  
675 on crystalline cellulose. *J Bacteriol* 179:6595-6601.
- 676 Garcia-Martinez DV, Shinmyo A, Madia A, and Demain AL. 1980. Studies on  
677 cellulase production by *Clostridium thermocellum*. *Eur J Appl Microbiol*  
678 *Biotechnol* 9:189-197.

- 679 Gilad R, Rabinovich L, Yaron S, Bayer EA, Lamed R, Gilbert HJ, and Shoham Y.  
680 2003. CellI, a non-cellulosomal family-9 enzyme from *Clostridium*  
681 *thermocellum*, is a processive endoglucanase that degrades crystalline  
682 cellulose. *J Bacteriol* 185:391-398.
- 683 Gilbert HJ, and Hazlewood GP. 1993. Bacterial cellulases and xylanases. *J Gen*  
684 *Microbiol* 139:187-194.
- 685 Gilbert HJ, Knox JP, and Boraston AB. 2013. Advances in understanding the  
686 molecular basis of plant cell wall polysaccharide recognition by carbohydrate-  
687 binding modules. *Current opinion in structural biology* 23:669-677.
- 688 Gilkes NR, Henrissat B, Kilburn DG, Miller RCJ, and Warren RAJ. 1991. Domains  
689 in microbial  $\beta$ -1,4-glycanases: sequence conservation, function, and enzyme  
690 families. *Microbiol Rev* 55:303-315.
- 691 Gruninger RJ, Gong X, Forster RJ, and McAllister TA. 2014. Biochemical and kinetic  
692 characterization of the multifunctional beta-glucosidase/beta-xylosidase/alpha-  
693 arabinosidase, Bgxa1. *Applied microbiology and biotechnology* 98:3003-3012.
- 694 Henrissat B. 1991. A classification of glycosyl hydrolases based on amino acid  
695 sequence similarities. *Biochem J* 280:309-316.
- 696 Henrissat B, and Davies G. 1997. Structural and sequence-based classification of  
697 glycoside hydrolases. *Curr Opin Struct Biol* 7:637-644.
- 698 Henrissat B, and Davies GJ. 2000. Glycoside hydrolases and glycosyltransferases.  
699 Families, modules, and implications for genomics. *Plant Physiol* 124:1515-  
700 1519.
- 701 Henrissat B, and Romeu A. 1995. Families, superfamilies and subfamilies of glycosyl  
702 hydrolases. *Biochem J* 311:350-351.
- 703 Irwin D, Shin D-H, Zhang S, Barr BK, Sakon J, Karplus PA, and Wilson DB. 1998.  
704 Roles of the catalytic domain and two cellulose binding domains of  
705 *Thermomonospora fusca* E4 in cellulose hydrolysis. *J Bacteriol* 180:1709-  
706 1714.
- 707 Jeon SD, Yu KO, Kim SW, and Han SO. 2012. The processive endoglucanase EngZ  
708 is active in crystalline cellulose degradation as a cellulosomal subunit of  
709 *Clostridium cellulovorans*. *New biotechnology* 29:365-371.
- 710 Kostylev M, Moran-Mirabal JM, Walker LP, and Wilson DB. 2012. Determination of  
711 the molecular states of the processive endocellulase *Thermobifida fusca*  
712 Cel9A during crystalline cellulose depolymerization. *Biotechnology and*  
713 *bioengineering* 109:295-299.
- 714 Krissinel E, and Henrick K. 2007. Inference of macromolecular assemblies from  
715 crystalline state. *J Mol Biol* 372:774--797.
- 716 Kuusk S, Sorlie M, and Valjamae P. 2015. The predominant molecular state of bound  
717 enzyme determines the strength and type of product inhibition in the  
718 hydrolysis of recalcitrant polysaccharides by processive enzymes. *The Journal*  
719 *of biological chemistry*.
- 720 Larkin MA, Blackshields G, Brown NP, Chenna R, McGettigan PA, McWilliam H,  
721 Valentin F, Wallace IM, Wilm A, Lopez R, Thompson JD, Gibson TJ, and  
722 Higgins DG. 2007. ClustalW and ClustalX version 2. *Bioinformatics* 23:2947-  
723 2948.
- 724 Li Y, Irwin DC, and Wilson DB. 2007. Processivity, substrate binding, and  
725 mechanism of cellulose hydrolysis by *Thermobifida fusca* Cel9A. *Appl*  
726 *Environ Microbiol* 73:3165-3172.
- 727 Li Y, Irwin DC, and Wilson DB. 2010. Increased crystalline cellulose activity via  
728 combinations of amino acid changes in the family 9 catalytic domain and

- 729 family 3c cellulose binding module of *Thermobifida fusca* Cel9A. *Appl*  
730 *Environ Microbiol* 76:2582-2588.
- 731 Lu H, Luo H, Shi P, Huang H, Meng K, Yang P, and Yao B. 2014. A novel  
732 thermophilic endo-beta-1,4-mannanase from *Aspergillus nidulans* XZ3:  
733 functional roles of carbohydrate-binding module and Thr/Ser-rich linker  
734 region. *Applied microbiology and biotechnology* 98:2155-2163.
- 735 Ma B, Tsai CJ, Haliloglu T, and Nussinov R. 2011. Dynamic allostery: linkers are not  
736 merely flexible. *Structure (London, England : 1993)* 19:907-917.
- 737 Mandelman D, Belaich A, Belaich JP, Aghajari N, Driguez H, and Haser R. 2003. X-  
738 Ray crystal structure of the multidomain endoglucanase Cel9G from  
739 *Clostridium cellulolyticum* complexed with natural and synthetic cello-  
740 oligosaccharides. *J Bacteriol* 185:4127-4135.
- 741 Matthews BW. 1968. Solvent content of protein crystals. *J Mol Biol* 33:491-497.
- 742 Meekins DA, Raththagala M, Husodo S, White CJ, Guo HF, Kotting O, Vander Kooi  
743 CW, and Gentry MS. 2014. Phosphoglucan-bound structure of starch  
744 phosphatase Starch Excess4 reveals the mechanism for C6 specificity.  
745 *Proceedings of the National Academy of Sciences of the United States of*  
746 *America* 111:7272-7277.
- 747 Miller GL. 1959. Use of dinitrosalicylic acid reagent for determination of reducing  
748 sugar. *Anal Biochem* 31:426-428.
- 749 Mingardon F, Bagert JD, Maisonnier C, Trudeau DL, and Arnold FH. 2011.  
750 Comparison of family 9 cellulases from mesophilic and thermophilic bacteria.  
751 *Applied and environmental microbiology* 77:1436-1442.
- 752 Moraïs S, Alber O, Barak Y, Hadar Y, Wilson DB, Lamed R, Shoham Y, and Bayer  
753 EA. 2012. Functional association of the catalytic and ancillary modules  
754 dictates enzymatic activity in glycoside hydrolase family 43  $\beta$ -xylosidase. *J*  
755 *Biol Chem* 287:9213-9221.
- 756 Murshudov GN, Vagin AA, and Dodson EJ. 1997. Refinement of macromolecular  
757 structures by the maximum-likelihood method. *Acta Crystallogr D* 53:240-  
758 255.
- 759 Ng TK, Weimer TK, and Zeikus JG. 1977. Cellulolytic and physiological properties  
760 of *Clostridium thermocellum*. *Arch Microbiol* 114:1-7.
- 761 Noach I, Alber O, Bayer EA, Lamed R, Levy-Assaraf M, Shimon LJW, and Frolow  
762 F. 2008. Crystallization and preliminary X-ray analysis of *Acetivibrio*  
763 *cellulolyticus* cellulosomal type II cohesin module: Two versions having  
764 different linker lengths. *Acta Cryst* F64:58-61.
- 765 Oliveira OV, Freitas LCG, Straatsma TP, and Lins RD. 2009. Interaction between the  
766 CBM of Cel9A from *Thermobifida fusca* and cellulose fibers. *Journal of*  
767 *Molecular Recognition* 22:38-45.
- 768 Otwinowski Z, and Minor W. 1997. Processing of X-ray diffraction data collected in  
769 oscillation mode. *Meth Enzymol*, 307-326.
- 770 Payne CM, Bomble YJ, Taylor CB, McCabe C, Himmel ME, Crowley MF, and  
771 Beckham GT. 2011. Multiple functions of aromatic-carbohydrate interactions  
772 in a processive cellulase examined with molecular simulation. *The Journal of*  
773 *biological chemistry* 286:41028-41035.
- 774 Payne CM, Resch MG, Chen L, Crowley MF, Himmel ME, Taylor LE, 2nd,  
775 Sandgren M, Stahlberg J, Stals I, Tan Z, and Beckham GT. 2013.  
776 Glycosylated linkers in multimodular lignocellulose-degrading enzymes  
777 dynamically bind to cellulose. *Proceedings of the National Academy of*  
778 *Sciences of the United States of America* 110:14646-14651.

- 779 Perrakis A, Morris R, and Lamzin VS. 1999. Automated protein model building  
780 combined with iterative structure refinement. *Nature Struct Biol* 6:458-463.
- 781 Petkun S, Jindou S, Shimon LJW, Rosenheck S, Bayer EA, Lamed R, and Frolow F.  
782 2010a. Structure of a family 3b' carbohydrate-binding module from the Cel9V  
783 glycoside hydrolase from *Clostridium thermocellum*: structural diversity and  
784 implications for carbohydrate binding. *Acta Crystallographica Section D-*  
785 *Biological Crystallography* 66:33-43.
- 786 Petkun S, Jindou S, Shimon LJW, Rosenheck S, Bayer EA, Lamed R, and Frolow F.  
787 2010b. Structure of a family 3b' carbohydrate-binding module from the Cel9V  
788 glycoside hydrolase from *Clostridium thermocellum*. Structural diversity and  
789 implications for carbohydrate binding. *Acta Cryst D* 66:33-43.
- 790 Sakon J, Irwin D, Wilson DB, and Karplus PA. 1997. Structure and mechanism of  
791 endo/exocellulase E4 from *Thermomonospora fusca*. *Nature Struct Biol*  
792 4:810-818.
- 793 Sammond DW, Payne CM, Brunecky R, Himmel ME, Crowley MF, and Beckham  
794 GT. 2012. Cellulase linkers are optimized based on domain type and function:  
795 insights from sequence analysis, biophysical measurements, and molecular  
796 simulation. *PloS one* 7:e48615.
- 797 Schwarz WH. 2001. The cellulosome and cellulose degradation by anaerobic bacteria.  
798 *Appl Microbiol Biotechnol* 56:634-649.
- 799 Schwarz WH, Zverlov VV, and Bahl H. 2004. Extracellular glycosyl hydrolases from  
800 Clostridia. *Advan Appl Microbiol* 56:215-261.
- 801 Shimon LJ, Pages S, Belaich A, Belaich JP, Bayer EA, Lamed R, Shoham Y, and  
802 Frolow F. 2000a. Structure of a family IIIa scaffoldin CBD from the  
803 cellulosome of *Clostridium cellulolyticum* at 2.2 Å resolution. *Acta*  
804 *Crystallogr D Biol Crystallogr* 56:1560-1568.
- 805 Shimon LJW, Pagès S, Belaich A, Belaich JP, Bayer EA, Lamed R, Shoham Y, and  
806 Frolow F. 2000b. Structure of a family IIIa scaffoldin CBD from the  
807 cellulosome of *Clostridium cellulolyticum* at 2.2 Å resolution. *Acta*  
808 *Crystallogr D Biol Crystallogr* 56:1560-1568.
- 809 Sonan GK, Receveur-Brechot V, Duez C, Aghajari N, Czjzek M, Haser R, and  
810 Gerday C. 2007. The linker region plays a key role in the adaptation to cold of  
811 the cellulase from an Antarctic bacterium. *The Biochemical journal* 407:293-  
812 302.
- 813 Srisodsuk M, Reinikainen T, Penttila M, and Teeri TT. 1993. Role of the interdomain  
814 linker peptide of *Trichoderma reesei* cellobiohydrolase I in its interaction with  
815 crystalline cellulose. *The Journal of biological chemistry* 268:20756-20761.
- 816 Stout GH, and Jensen LH. 1968. *X-ray structure determination. A practical guide.*  
817 London: MacMillan.
- 818 Su X, Mackie RI, and Cann IK. 2012. Biochemical and mutational analyses of a  
819 multidomain cellulase/mannanase from *Caldicellulosiruptor bescii*. *Applied*  
820 *and environmental microbiology* 78:2230-2240.
- 821 Telke AA, Ghatge SS, Kang SH, Thangapandian S, Lee KW, Shin HD, Um Y, and  
822 Kim SW. 2012. Construction and characterization of chimeric cellulases with  
823 enhanced catalytic activity towards insoluble cellulosic substrates.  
824 *Bioresource technology* 112:10-17.
- 825 Tina KG, Bhadra R, and Srinivasan N. 2007. PIC: Protein interactions calculator.  
826 *Nucl Acids Res* 35:W473-W476.
- 827 Ting CL, Makarov DE, and Wang ZG. 2009. A kinetic model for the enzymatic  
828 action of cellulase. *The journal of physical chemistry B* 113:4970-4977.

- 829 Tormo J, Lamed R, Chirino AJ, Morag E, Bayer EA, Shoham Y, and Steitz TA. 1996.  
830 Crystal structure of a bacterial family-III cellulose-binding domain: A general  
831 mechanism for attachment to cellulose. *EMBO J* 15:5739-5751.
- 832 Vagin A, and Teplyakov A. 1997. MOLREP: an automated program for molecular  
833 replacement. *J Appl Crystallogr* 30:1022-1025.
- 834 Venditto I, Najmudin S, Luis AS, Ferreira LM, Sakka K, Knox JP, Gilbert HJ, and  
835 Fontes CM. 2015. Family 46 Carbohydrate-Binding Modules contribute to the  
836 enzymatic hydrolysis of xyloglucan and beta-1,3-1,4-glucans through distinct  
837 mechanisms. *The Journal of biological chemistry*.
- 838 Wiegel J, Mothershed CP, and Puls J. 1985. Differences in xylan degradation by  
839 various noncellulolytic thermophilic anaerobes and *Clostridium thermocellum*.  
840 *Appl Environ Microbiol* 49:656-659.
- 841 Wilson DB, and Irwin DC. 1999. Genetics and properties of cellulases. *Adv Biochem*  
842 *Eng* 65:1-21.
- 843 Wilson DB, and Kostylev M. 2012. Cellulase processivity. *Methods in molecular*  
844 *biology (Clifton, NJ)* 908:93-99.
- 845 Winn MD, Isupov MN, and Murshudov GN. 2001. Use of TLS parameters to model  
846 anisotropic displacements in macromolecular refinement. *Acta Crystallogr D*  
847 57:122-133.
- 848 Winn MD, Murshudov GN, and Papiz MZ. 2003. Macromolecular TLS refinement in  
849 REFMAC at moderate resolution. *Methods Enzymol* 374:300-321.
- 850 Yaniv O, Fichman G, Borovok I, Shoham Y, Bayer EA, Lamed R, Shimon LJ, and  
851 Frolow F. 2014. Fine-structural variance of family 3 carbohydrate-binding  
852 modules as extracellular biomass-sensing components of *Clostridium*  
853 *thermocellum* anti-sigma factors. *Acta crystallographica Section D,*  
854 *Biological crystallography* 70:522-534.
- 855 Yaniv O, Frolow F, Levy-Assraf M, Lamed R, and Bayer EA. 2012a. Interactions  
856 between family 3 carbohydrate binding modules (CBMs) and cellulosomal  
857 linker peptides. *Methods in enzymology* 510:247-259.
- 858 Yaniv O, Petkun S, Shimon LJ, Bayer EA, Lamed R, and Frolow F. 2012b. A single  
859 mutation reforms the binding activity of an adhesion-deficient family 3  
860 carbohydrate-binding module. *Acta crystallographica Section D, Biological*  
861 *crystallography* 68:819-828.
- 862 Yaniv O, Shimon LJ, Bayer EA, Lamed R, and Frolow F. 2011. Scaffoldin-borne  
863 family 3b carbohydrate-binding module from the cellulosome of *Bacteroides*  
864 *cellulosolvens*: structural diversity and significance of calcium for  
865 carbohydrate binding. *Acta crystallographica Section D, Biological*  
866 *crystallography* 67:506-515.
- 867 Yi Z, Su X, Revindran V, Mackie RI, and Cann I. 2013. Molecular and biochemical  
868 analyses of CbCel9A/Cel48A, a highly secreted multi-modular cellulase by  
869 *Caldicellulosiruptor bescii* during growth on crystalline cellulose. *PloS one*  
870 8:e84172.
- 871 Zhou W, Irwin DC, Escovar-Kousen J, and Wilson DB. 2004. Kinetic studies of  
872 *Thermobifida fusca* Cel9A active site mutant enzymes. *Biochemistry* 43:9655-  
873 9663.
- 874 Zmudka MW, Thoden JB, and Holden HM. 2013. The structure of DesR from  
875 *Streptomyces venezuelae*, a beta-glucosidase involved in macrolide activation.  
876 *Protein science : a publication of the Protein Society* 22:883-892.
- 877 Zverlov VV, Velikodvorskaya GA, and Schwarz WH. 2003. Two new cellulosome  
878 components encoded downstream of *celI* in the genome of *Clostridium*

879 *thermocellum*: the non-processive endoglucanase CelN and the possibly  
880 structural protein CseP. *Microbiology* 149:515-524.  
881  
882  
883

884

**Table 1** Diffraction data of the GH9-CBM3c *in vitro* reassembled complex from Cel9I from *C. thermocellum*. Values shown in parentheses are for the highest resolution cell.

GH9-CBM3c	ESRF
Space group	P2 <sub>1</sub> 2 <sub>1</sub> 2 <sub>1</sub>
Number of crystals	1
Total rotation range (°)	240
<i>a</i> (Å)	70.39
<i>b</i> (Å)	88.54
<i>c</i> (Å)	106.49
<i>V</i> (Å <sup>3</sup> )	663743.40
Resolution range (Å)	30-1.68 (1.71-1.68)
Total number of reflections	676571
Unique reflections	76727
Mosaicity range (°)	0.18-0.46
Average redundancy	9.0
Completeness, overall (%)	97.9 (74.8)
Mean <i>I</i> / $\sigma$ ( <i>I</i> )	34.72 (2.08)
<i>R</i> <sub>merge</sub> <sup>†</sup> (%)	7.4 (49.8)

885

886 <sup>†</sup>  $R_{\text{merge}} = \frac{\sum_{hkl} \sum_i |I_i(hkl) - \langle I(hkl) \rangle|}{\sum_{hkl} \sum_i I_i(hkl)}$ , where  $\sum_{hkl}$  denotes the sum over all reflections and  $\sum_i$  the sum  
 887 over all equivalent and symmetry-related reflections. (Stout & Jensen 1968)

888

889

890

891

892

893

894

**Table 2** Refinement statistics and results of *MolProbity* validation

†Clash score is the number of serious steric overlaps (&gt; 0.4 Å) per 1000 atoms.

Protein	Reassembled GH9 and CBM3c (Cel9I)
Space group	P2 <sub>1</sub> 2 <sub>1</sub> 2 <sub>1</sub>
Resolution range	30-1.68
No. of reflections in working set	71559
No. of reflections in test set	3580
No. of protein atoms	5071
No. of solvent atoms	835
No. of Cl ion atoms	3
No. of Ca ion atoms	2
Overall B factor from Wilson plot (Å <sup>2</sup> )	16.06
Averaged B factor (Å <sup>2</sup> )	21.12
R <sub>cryst</sub>	0.1441
R <sub>free</sub>	0.1759
<b>Geometry</b>	
RMS bonds (Å)	0.014
RMS bond angles (°)	1.371
<b>MolProbity validation</b>	
Ramachandran favored (%) (goal >98%)	96.7
Ramachandran outliers (%) (goal <0.2%)	0.5
C <sub>β</sub> deviations >0.25Å (goal 0)	1
† Clash score (all atoms)	2.88
Rotamer outliers (%) (goal <1%)	0.8
Residues with bad bonds (%) (goal <1%)	0.00
Residues with bad angles (%) (goal <0.5)	0.33

895

896

897

898 **Figure captions:**

899 **Figure 1.** Schematic diagram of the Cel9I gene product (top) and the recombinant  
900 proteins (A-D) prepared for this study. The GH9 module alone (B) was prepared with  
901 and without an N-terminal His tag (shown schematically in the figure), and the  
902 CBM3c's were prepared with C-terminal His tags. Scale shows the number of amino  
903 acid residues and the boundaries of the different regions of the protein.

904 **Figure 2.** Recovery of activity upon association of CBM3c (with and without linker)  
905 and GH9. CMCase activity ( $\mu\text{mol}$  reducing sugar released in a 10-min reaction) of  
906 His-tagged GH9, mixed either with CBM3c $L$  (diamonds) or CBM3c $NL$  (squares),  
907 was examined. A fixed amount (70 pmol) of the GH9 catalytic module was mixed  
908 with increasing amounts of the indicated helper module, and their respective activities  
909 were compared to that of the intact Cel9I core (GH9-CBM3c, set as 100%).

910 **Figure 3.** Reassembled GH9-CBM3c from Cel9I. C and N termini are indicated,  
911 and the break between the GH9 and CBM3c modules is marked by a red ellipse. A.  
912 The *in vitro* reassembled complex of the catalytic (GH9, wheat) and carbohydrate-  
913 binding (CBM3c, green) modules of Cel9I from *C. thermocellum*, cartoon  
914 representation. Calcium atoms are shown as magenta-colored spheres. B. Stereo-view  
915 (cross-eyed) of the superposition of the reassembled GH9-CBM3c structure of *C.*  
916 *thermocellum* Cel9I (red) with the bimodular structures of *C. cellulolyticum* Cel9G  
917 (blue) and *T. fusca* Cel9A (green).

918 **Figure 4.** Structural components of the reassembled *C. thermocellum* GH9-CBM3c.  
919 A. Structure of the GH9 catalytic module, cartoon representation. Twelve  $\alpha$ -helices  
920 form an  $(\alpha/\alpha)_6$ -barrel fold. Pairs of helices, comprising the fold, are emphasized by  
921 red, blue, yellow, magenta, cyan and green. B. Surface representation of the  
922 reassembled GH9-CBM3c complex. The residues are shaded according to the extent  
923 of their conservation with Cel9G from *C. cellulolyticum* and Cel9A from *T. fusca*.  
924 Darker blue indicates higher conservation. Top, birds-eye view of the catalytic cleft.  
925 Bottom, lateral view, showing the flat surface (red bar). Pink ellipse indicates the  
926 catalytic cleft, and green ellipse designates terminal portion of the catalytic site. C.  
927 Close-up (same orientation as in B, top) of the catalytic cleft of the Cel9I GH9  
928 module showing functional residues. Carbohydrate-binding residue carbons are  
929 colored gray, catalytic residue carbons are colored yellow. Loop 243-254 carbons are

930 colored in light blue. D. Calcium-binding site of the *C. thermocellum* Cel9I GH9  
931 module. Coordinating residues are shown in stick representation. The calcium ion is  
932 colored magenta, and distances to the coordinating atoms are indicated.

933 **Figure 5.** Structure of the CBM3c of Cel9I from *C. thermocellum*. C and N termini  
934 are indicated A. Cartoon representation,  $\beta$ -strands are numbered according to the  
935 alignment with Cel9G from *C. cellulolyticum*, and Cel9A from *T. fusca*. B. Calcium-  
936 binding site of the CBM3c. C. Birds-eye view of the flat surface. Residues are shaded  
937 according to their degree of conservation with *C. cellulolyticum* Cel9G and *T. fusca*  
938 CEL9A. Surface-exposed conserved residues are shown in stick representation. D.  
939 Shallow groove of the CBM3c. Conserved surface residues are shown in stick  
940 representation. The residues are colored according to the degree of conservation in  
941 CBM3a, CBM3b and CBM3c modules derived from the sequences listed in the  
942 Methods section.

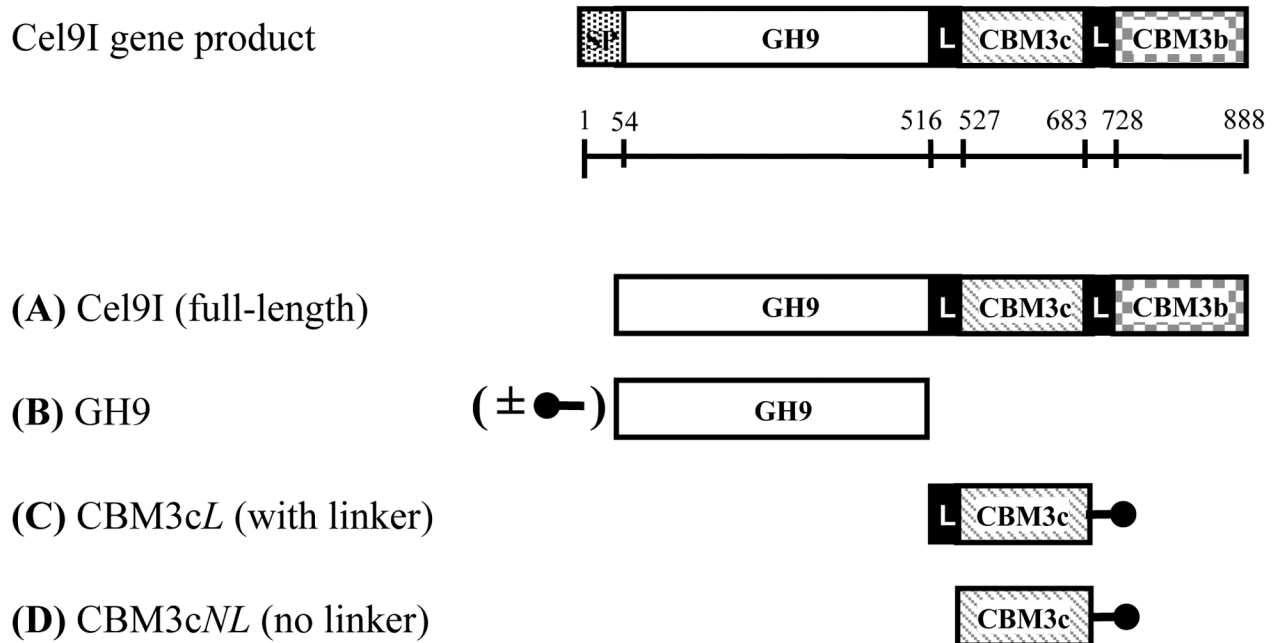
943 **Figure 6.** Contact residues of the reassembled GH9-CBM3c complex. A. Contact  
944 residues of the GH9 module are colored orange, of the CBM3c module green. Contact  
945 residues between the linker and the catalytic domain are indicated (in green: CBM3c  
946 residues, in brown: GH9 residues). B. Alignment of the GH9 and CBM3c modules of  
947 *C. thermocellum* Cel9I, *C. cellulolyticum* Cel9G, and *T. fusca* Cel9A (E4) cellulases.  
948 Contact residues are highlighted in yellow. Only the relevant regions of the alignment  
949 are shown. Residues of linker sequences are shown blue font.

950 **Figure 7.** Representative ITC titration of (A) GH9 and CBM3c<sub>NL</sub> (B) GH9 and  
951 CBM3c<sub>L</sub>. The top panel shows the calorimetric titration and the bottom panel  
952 displays the integrated injection heats corrected for control dilution heat. The solid  
953 line is the curve of the best fit used to derive the binding parameters, and the fitted  
954 data describe an interaction of a one binding site model.

955

956 **Figure 1. Schematic diagram of the Cel9I gene product and the recombinant**  
 957 **proteins prepared for this study**

958



959

960

961

962

963

964

965 **Figure 1.** Schematic diagram of the Cel9I gene product (top) and the recombinant  
 966 proteins (A-D) prepared for this study. The GH9 module alone (B) was prepared with  
 967 and without an N-terminal His tag (shown schematically in the figure), and the  
 968 CBM3c's were prepared with C-terminal His tags. Scale shows the number of amino  
 969 acid residues and the boundaries of the different regions of the protein.

970

971 **Figure 2. Recovery of activity upon association of CBM3c (with and without linker) and**  
972 **GH9.**

973

974

975

976

977

978

979

980

981

982

983

984

985

986

987

988

989

990 Figure 2. Recovery of activity upon association of CBM3c (with and without linker)

991 and GH9. CMCase activity ( $\mu\text{mol}$  reducing sugar released in a 10-min reaction) of

992 His-tagged GH9, mixed either with CBM3cL (diamonds) or CBM3cNL (squares),

993 was examined. A fixed amount (70 pmol) of the GH9 catalytic module was mixed

994 with increasing amounts of the indicated helper module, and their respective activities

995 were compared to that of the intact Cel9I (set as 100%).

996

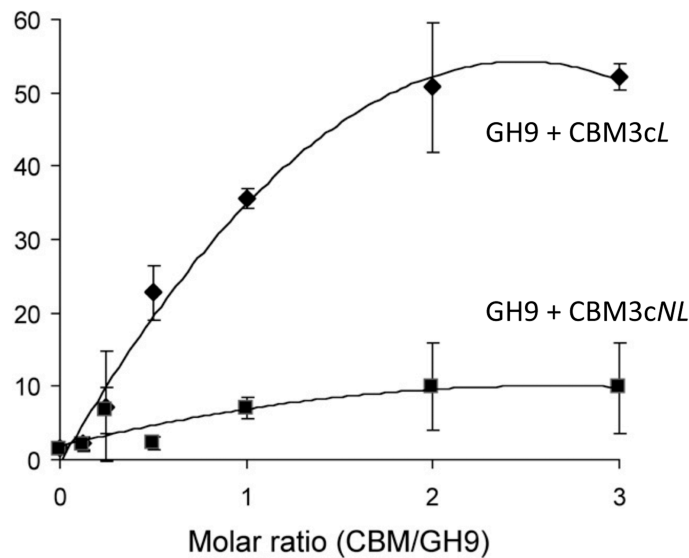
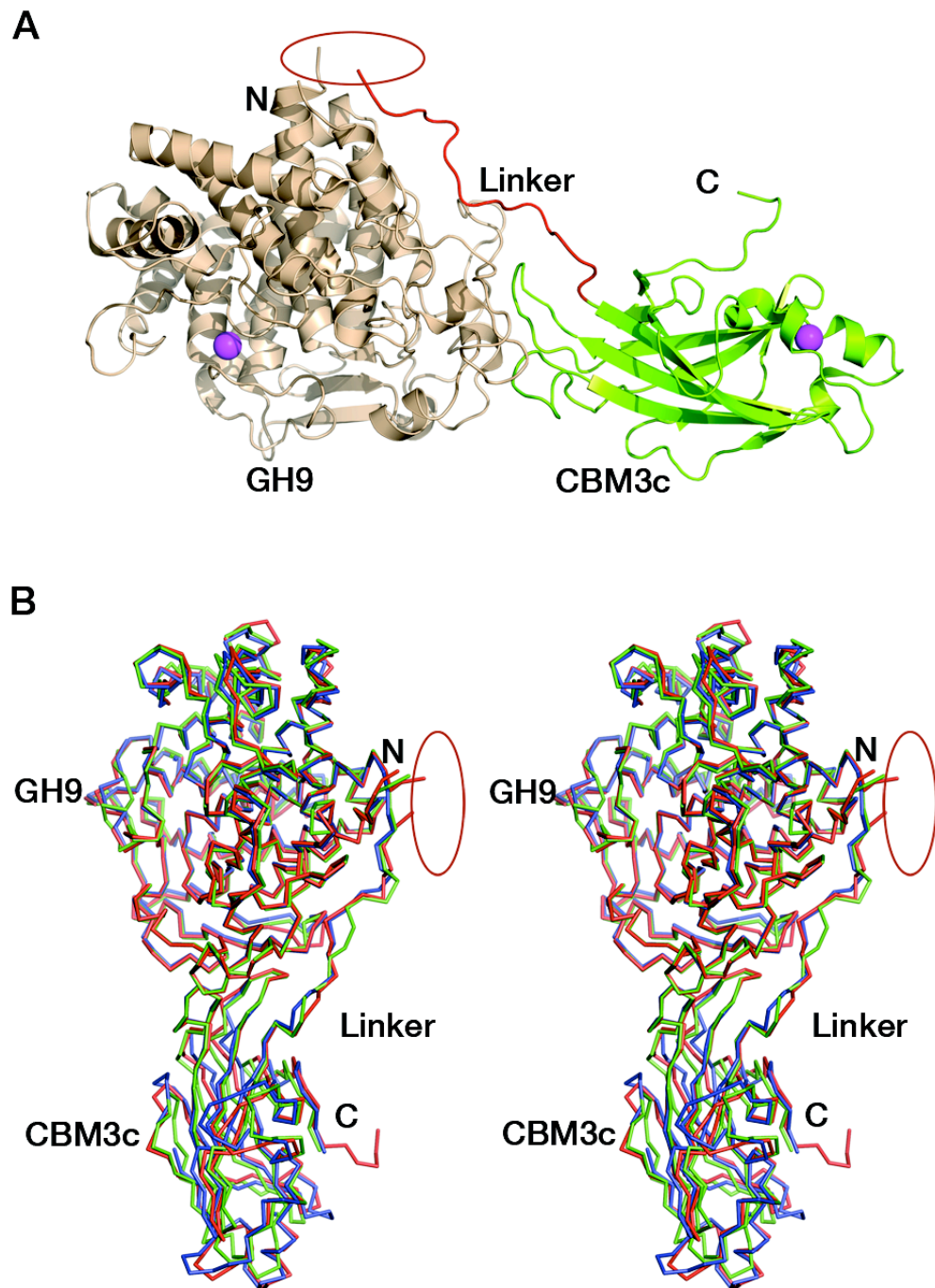
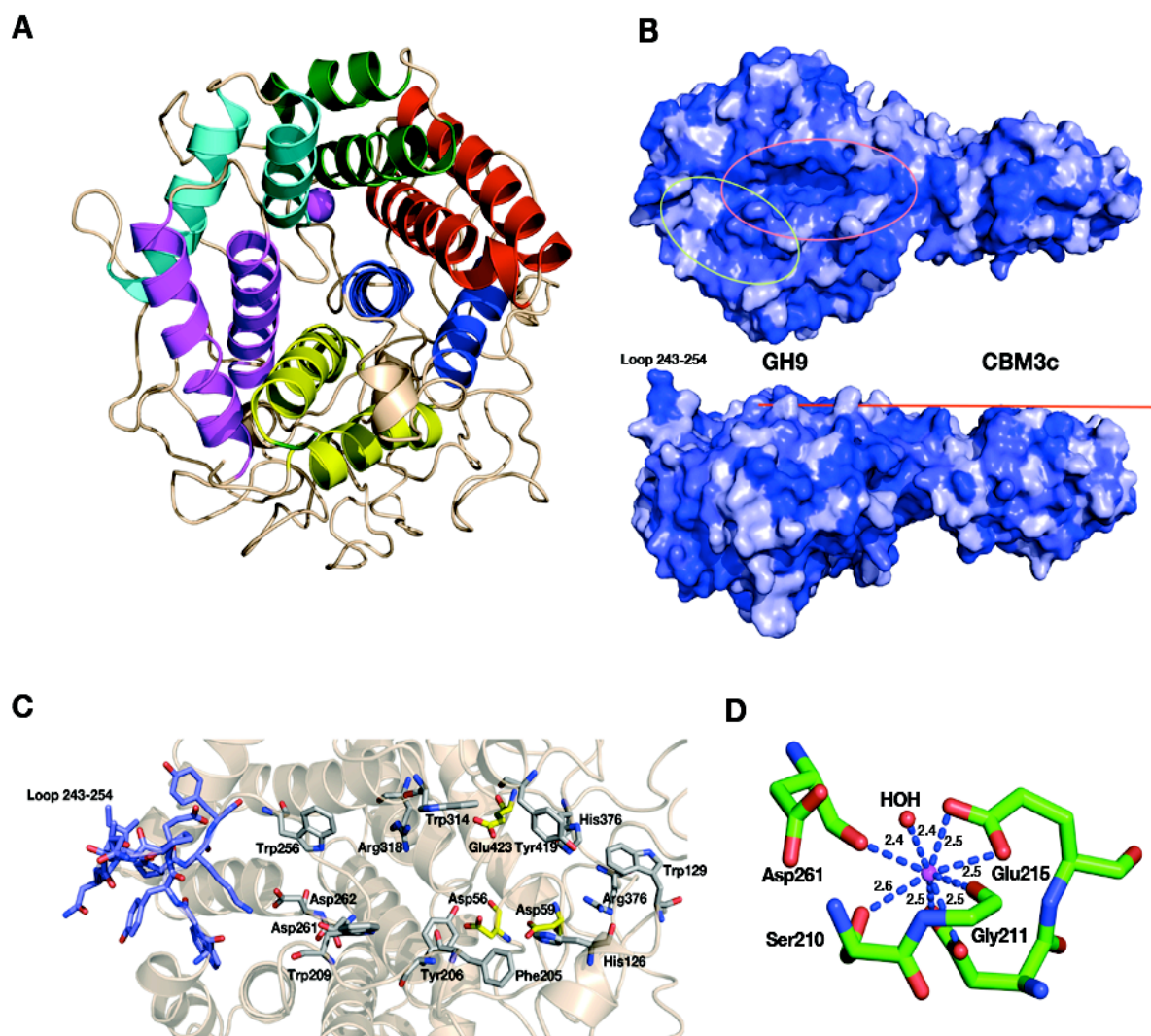


Figure 3. Reassembled GH9-CBM3c from Cel9I.



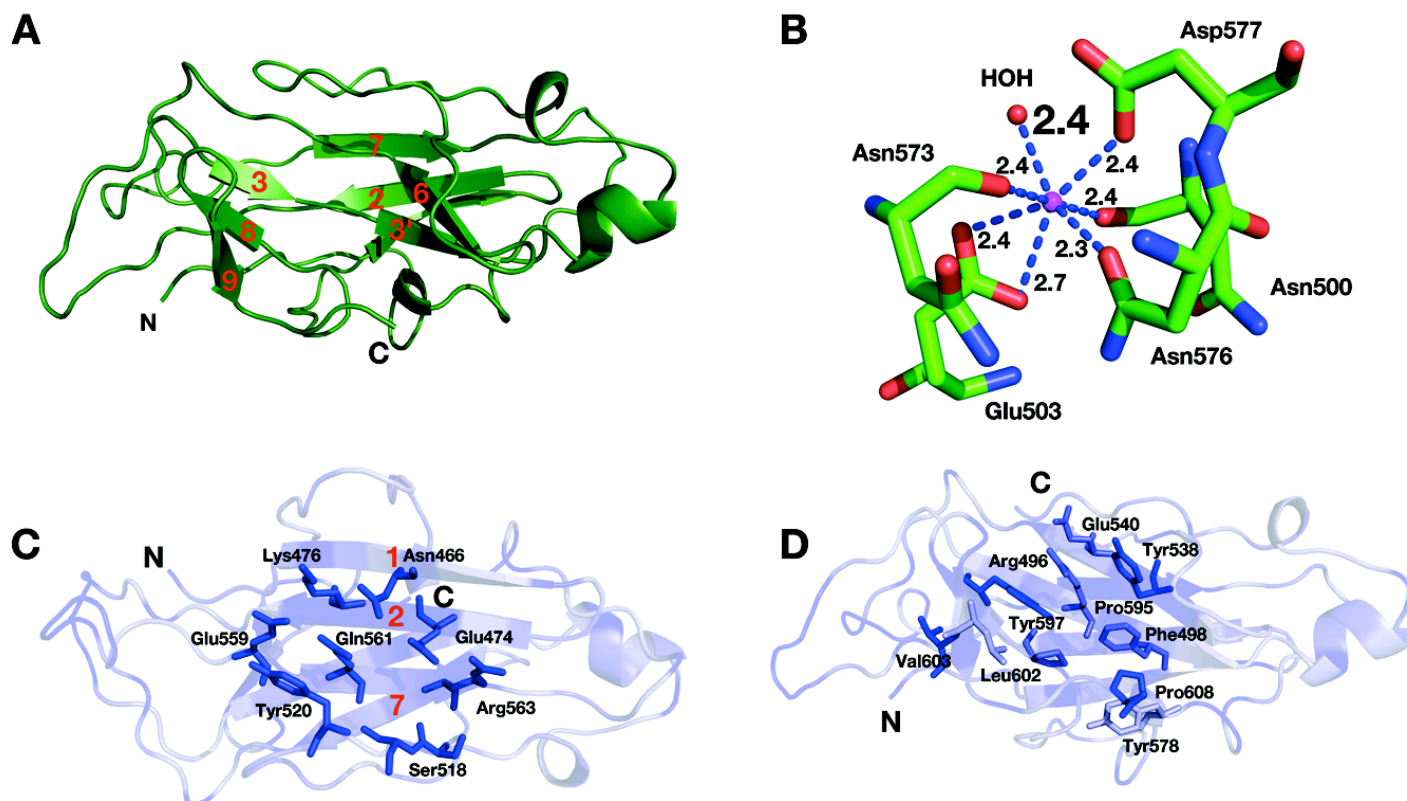
1026 Figure 3. Reassembled GH9-CBM3c from Cel9I. C and N termini are indicated, and  
1027 the break between the GH9 and CBM3c modules is marked by a red ellipse. A. The  
1028 *in vitro* reassembled complex of the catalytic (GH9, wheat) and carbohydrate-binding  
1029 (CBM3c, green) modules of Cel9I from *C. thermocellum*, cartoon representation.  
1030 Calcium atoms are shown as magenta-colored spheres. B. Stereo-view (cross-eyed)  
1031 of the superposition of the reassembled GH9-CBM3c structure of *C. thermocellum*  
1032 Cel9I (red) with the bimodular structures of *C. cellulolyticum* Cel9G (blue) and *T.*  
1033 *fusca* Cel9A (green).

1034

1035 **Figure 4. Structural components of the reassembled GH9-CBM3c.**

1036  
 1037  
 1038  
 1039  
 1040  
 1041  
 1042  
 1043  
 1044  
 1045  
 1046  
 1047  
 1048  
 1049  
 1050  
 1051  
 1052  
 1053  
 1054

**Figure 4.** Structural components of the reassembled GH9-CBM3c. A. Structure of the GH9 catalytic module, cartoon representation. Twelve  $\alpha$ -helices form an  $(\alpha/\alpha)_6$ -barrel fold. Pairs of helices, comprising the fold, are emphasized by red, blue, yellow, magenta, cyan and green. B. Surface representation of the reassembled GH9-CBM3c complex. The residues are shaded according to the extent of their conservation with Cel9G from *C. cellulolyticum* and Cel9A from *T. fusca*. Darker blue indicates higher conservation. Top, birds-eye view of the catalytic cleft. Bottom, lateral view, showing the flat surface (red bar). Pink ellipse indicates the catalytic cleft, and green ellipse designates terminal portion of the catalytic site. C. Close-up (same orientation as in B, top) of the catalytic cleft of the Cel9I GH9 module showing functional residues. Carbohydrate-binding residue carbons are colored gray, catalytic residue carbons are colored yellow. Loop 243-254 carbons are colored in light blue. D. Calcium-binding site of the *C. thermocellum* Cel9I GH9 module. Coordinating residues are shown in stick representation. The calcium ion is colored magenta, and distances to the coordinating atoms are indicated.

1055 **Figure 5.** Structure of the CBM3c of Cel9I from *C. thermocellum*.

1056

1057

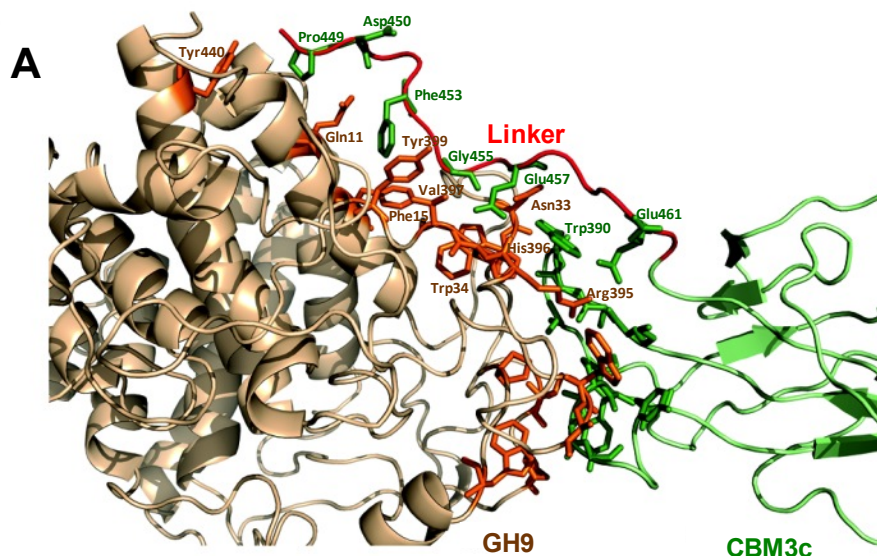
1058

1059

1060 **Figure 5.** Structure of the CBM3c of Cel9I from *C. thermocellum*. C and N termini  
 1061 are indicated A. Cartoon representation,  $\beta$ -strands are numbered according to the  
 1062 alignment with Cel9G from *C. cellulolyticum*, and Cel9A from *T. fusca*. B. Calcium-  
 1063 binding site of the CBM3c. C. Birds-eye view of the flat surface. Residues are shaded  
 1064 according to their degree of conservation with *C. cellulolyticum* Cel9G and *T. fusca*  
 1065 CEL9A. Surface-exposed conserved residues are shown in stick representation. D.  
 1066 Shallow groove of the CBM3c. Conserved surface residues are shown in stick  
 1067 representation. The residues are colored according to the degree of conservation in  
 1068 CBM3a, CBM3b and CBM3c modules derived from the sequences listed in the  
 1069 Methods section.

1070

1071 **Figure 6. Contact residues of the reassembled GH9-CBM3c complex.**  
 1072  
 1073



**B**      **GH9 Modules**

```

CelI  gAFNYGEALQKAIFFYECQRSGKLDPsTLRLNWRGDSGLDDGKDAGIDLTGGWYDAGDHV   60
CelG  .TNYNGEALQKSIMFYEFQRSGLDPA.DKRDNWRDDSGMKDGSVDVGLTGGWYDAGDHV   58
E4    PAFNYAEALQKSMFFYEAQRSGLKP.ENNRVSWRGDSGLNDGADVGLDLTGGWYDAGDHV   60
  
```

```

-----
CelI  GHADHAWWGPAEVMQMERPSYKVDRSSPGSTVVAETSAAALAIASIIFFKKVDGEYSKECLK   180
CelG  GGDHSHWVGPAEVMQMERPSFKVDASKPGSAVCASTAASLASAAVVFKSSDPTYAECIS     178
E4    GDADHKWVGPAEVMQMERPSFKVDSPCPGSDVAAETAAMAASSIVFADDDPAYAATLVQ     180
  
```

```

-----
CelI  GRSFVVGFGENPPKRPHHRTAHGSWADSQMEPPEHRHVLYGALVGGP.DSTDNYTDDISN     420
CelG  GRSFVVGYGVPQPHHRTAHGSWTDQMTSPTYHRHTIYGALVGGP.DNADGYTDEINN     416
E4    NSSYVVGFGNPPRPHHRTAHGSWTDSIASPAENRHVLYGALVGGPqSPNDAYTDDRQD     422
  
```

```

-----
CelI  YTCNEVACDYNAGFVGLLAKMYKLYGE   444
CelG  YVNNEIACDYNAGFTGALAKMYKHSGG   440
E4    YVANEVATDYNAGFSSALAMLVVEEYG.   445
  
```

**CBM3c Modules**

```

CelI  SPDPKFNGIEEVPDEIFVEAGVNASGNFIEIKAIVNNKSGWPARVCENLSFRYFINIE   60
CelG  DPIPNEKAIKAITNDEVIKAGLNSTGPNYTEIKAVVYNQTGWPARVTDKISFKYFMDLS   60
E4    TPLADEFPTEEPDQPEIFVEAQINTPGTTFTEIKAMIRNOSGWPARMLDKGTFRYWFTLD   61
  
```

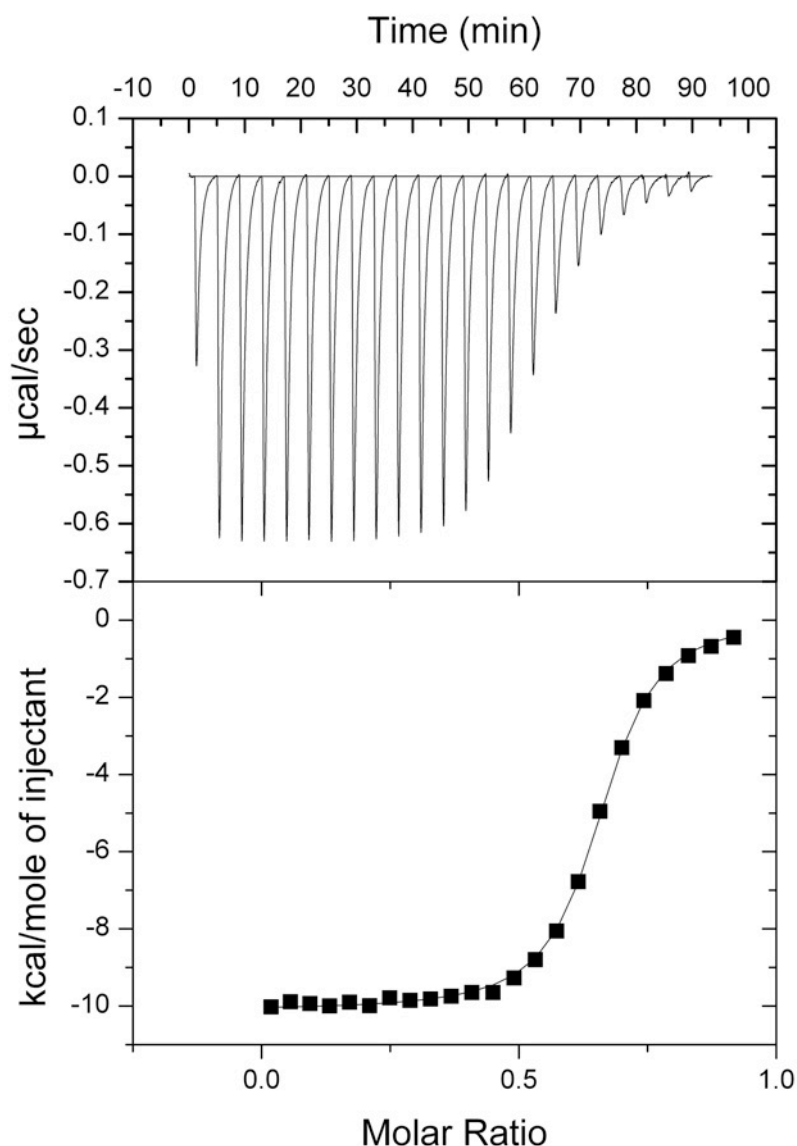
```

CelI  EIVNAGKSASDLQVSSsYNQG..AKLS.DVKHYK..DNIYYVEVDLSGTKIYPGGQSAKK   116
CelG  EIVAAGIDPLSLVTSS.YSEGknTKVS.GVLPWDvsNNVYYVNVDLTGENIYPGGQSACRR   119
E4    EGV...DPADITVSSAYNQ...CATPeDVHHVS..GDLYYVEIDCTGEKIFPGGQSEHRR   111
  
```

1074

1075

1076 **Figure 6.** Contact residues of the reassembled GH9-CBM3c complex. A. Contact  
 1077 residues of the GH9 module are colored orange, of the CBM3c module green. Contact  
 1078 residues between the linker and the catalytic domain are indicated (in green: CBM3c  
 1079 residues, in brown: GH9 residues). B. Alignment of the GH9 and CBM3c modules of  
 1080 *C. thermocellum* Cel9I, *C. cellulolyticum* Cel9G, and *T. fusca* Cel9A (E4) cellulases.  
 1081 Contact residues are highlighted in yellow. Only the relevant regions of the alignment  
 1082 are shown. Residues of linker sequences are shown blue font.

1083 **Figure 7. Representative ITC titration of GH9 and CBM3cNL.**

1084

1085

1086

1087

1088

1089

1090

1091 Figure 7. Representative ITC titration of GH9 and CBM3cNL. The top panel shows

1092 the calorimetric titration and the bottom panel displays the integrated injection heats

1093 corrected for control dilution heat. The solid line is the curve of the best fit used to

1094 derive the binding parameters, and the fitted data describe an interaction of a one

1095 binding site model.

1096

1097

1098